# *Leishmania major* formins are cytosolic actin bundler play an important role in cell physiology

**Renu Kushwaha[1]*, Arunava Seth[1]*, A.S. Jijumon[1], Reshmi P.B[1]., Drisya Dileep[1], Rupak Datta[1#] and Sankar Maiti[1#]**

[1]Department of Biological Sciences, Indian Institute of Science Education and Research Kolkata, Mohanpur, - 741246, Nadia, West Bengal, India

*(contributed equally)

[#] Contributed equally
Correspondence:
Sankar Maiti (PhD)
Rupak Datta (PhD) rupakdatta@iiserkol.ac.in
Indian Institute of Science Education and Research Kolkata
Mohanpur, Nadia - 741246
West Bengal, India
Email: spm@iiserkol.ac.in

## ABSTRACT

Formin proteins regulate actin dynamics, are conserved throughout the eukaryotes cells. They play an important role in cell adhesion, motility, vesicular trafficking, and cytokinesis. Formins from class Kinetoplastida which includes infective organisms such as *Leishmania* and *Trypanosoma* not characterized to date, even though they are shown to be important in other protozoan parasites. The protozoan parasite *Leishmania major (Lm)* has two homologous formin proteins; LmForminA and LmForminB. Our study showed that LmForminA and LmForminB are expressed at RNA and protein levels in *L. major* cells. LmForminA and LmForminB are localized in the cytosol in patchy distribution patterns. LmForminA and LmForminB puncta also colocalize with the actin patches. The biochemical properties of *L. major* formins divulge that both formins are potent actin nucleator. LmForminA and LmForminB bind with the actin filament and have actin-bundling

activity. We have also observed that formin inhibitor SMIFH2 influences the growth and physiology of *L. major* cells indicating formins are important for the Leishmania parasite.

**KEYWORDS**

Leishmania, formin, actin dynamics, actin bundling

## INTRODUCTION

Leishmaniasis is caused by the intracellular protozoan parasite *Leishmania sp.* affects more than 12 million people worldwide with 20,000-40,000 deaths annually, making it one of the most severe tropical neglected diseases (Okwor and Uzonna, 2016). The unavailability of vaccine and the rise of drug-resistant *Leishmania* species calls for the development of new therapeutics, emphasizing the need to study the parasite's cellular mechanisms with greater impetus (Ponte-Sucre *et al*., 2017). The parasite follows a digenetic lifestyle in mammalian hosts (such as humans), and the insect vector (Sandfly) exists in two distinct forms in the two separate hosts. The motile elongated promastigotes with long flagella in sandfly vector and as non-motile rounded amastigote form, which resides in host macrophage (Chow *et al*., 2011; Tsigankov *et al*., 2014). Cytoskeleton restructuring of the parasite involved in the motility and the entry in the host cells are the crucial events for the successful infection and the survival of the parasite in the phagosome (Frenal and Soldati-Favre, 2009). The decrease in cell size is probably to decrease the surface to volume ratio of the parasite to minimize contact with harsh parasitophorous vacuole (Sunter and Gull, 2017). The cytoskeletal restructuring event and range of physiological and cytological changes in *Leishmania* physiology are yet to be understood properly (Goyard *et al*., 2003). *Leishmania* cytoskeleton is known to contain actin along with microtubule and intermediate filaments (Gull, 1999).

*Leishmania* actin is present in the cytoplasm, flagella, flagellar pocket, nucleus and kinetoplast, shares 69.8% identity with the mammalian actin (Sahasrabuddhe, Bajpai and Gupta, 2004). Actin is also present on the nuclear, vacular, and cytoplasmic face of plasma membranes (Sahasrabuddhe, Bajpai and Gupta, 2004). *Leishmania* actin plays a vital role in cellular processes like microtubule-actin associated vesicle transport, organelle movement, endocytosis, basal body separation, and flagellar pocket division (Sahasrabuddhe, Bajpai and Gupta, 2004; Tammana et al., 2010). Some actin-binding proteins such as profilin, Arp2/3 protein, cofilin, and coronin are reported in *Leishmania*, which are involved in different cellular functions from cell division to vesicular trafficking, indicating the importance of actin in *Leishmania* physiology (Nayak *et al.*, 2005; Tammana *et al*., 2010). However, the functional aspect of an important class of actin-nucleating protein, that is, formins in *Leishmania*, remains elusive to date.

Formin class of proteins are long multi-domain proteins (Castrillon and Wasserman, 1994; Zeller et al., 1999). FH1, FH2 and FH3 are formin homology domains present in most of the formin family of proteins. FH1 domain is a polyproline-rich region present proximately to the FH2 domain. The binding of the profilin-actin complex with the FH1 region promotes the continuous addition of actin monomer molecule on actin filament growing end (Kovar and Pollard, 2004; Romero *et al.,* 2007). The FH3 domain plays a role in the formin localization in the cell (Petersen *et al*., 1998; Kato *et al*., 2001). Formin has a conserved FH2 domain contain around 400 amino acid residues (Kovar and Pollard, 2004; Romero *et al*., 2007). Formin FH2 domain binds with actin molecules to help actin filaments nucleation and elongation (Pruyne *et al*., 2002; Sagot, Klee and Pellman, 2002). Formins FH2 domain binding with filament barbed end protects from complete inhibition by the capping protein (Kovar and Pollard, 2004).

Phylogenetic analysis of formins described that formin is a multigene family protein (Cvrcková *et al*., 2004; Li and Higgs, 2005; Rivero *e*t al., 2005; Wasserman, 1998). Multiple formin genes are present throughout the eukaryotes, such as *Plasmodium falciparum* (2 genes), *Toxoplasma gondii* (3 genes), *Caenorhabditis elegans* (6 genes), *Dictyostelium discoideum* (10 genes), *Schizosaccharomyces pombe* (3 genes), *Saccharomyces cerevisiae* (2 genes), *Drosophila melanogaster* (6 genes), and mammals (15 genes) (Chalkia *et al*., 2008).

Biochemical and cellular characterization reveals the necessity of these formin families in eukaryotes. *In vivo* studies of *Saccharomyces cerevisiae* formins, Bnip, and Bn1p shows their role in cytokinetic actin ring and actin cable assembly (Evangelista *et al*., 2002; Sagot, Klee and Pellman, 2002). Loss of both the formin genes in *S. cerevisiae* shows lethality (Ozaki-Kuroda *et al*., 2001). The Bni1p and Bnr1p formin's biochemical functions are actin filament nucleation; additionally, bnr1 is an F-actin bundler but not bni1 (Moseley and Goode, 2005). Some formins from protozoa like *Chlamydomonas, Entamoeba. histolytica, Toxoplasma, and Plasmodium* also have been characterized. *Chlamydomonas reinhardtii* formin CrFor1 nucleates actin molecules and helps in fertilization tubule formation in Chlamydomonas (Christensen *et al*., 2019).

*Entamoeba formin* isoform Ehformin-1 and -2 binds with the F-actin structures and involves in cellular processes like motility, phagocytosis and cell division (Majumder and Lohia, 2008). *Toxoplasma gondii* formins contribute to parasite movement and help in the host cell invasion (Daher *et al*., 2010; Daher *et al*., 2012). Recently it has been found that formin-2 in *Plasmodium falciparum* and *Toxoplasma gondii* play a vital role in apicoplast segregation (Stortz *et al*., 2019). *Plasmodium falciparum* Formin-1(PfFormin1) and formin-2 (PfFormin2) has actin polymerization. The Pf1 has been reported to have a role in invasion (Baum et al., 2008).

Such a diverse role of these formin in parasite groups brings our attention towards a very primitive organism, *L. major*, which was thought to be evolved 80 million years ago (Chalkia *et al*., 2008). The flagellated protozoan parasite belongs to the Kinetoplastida group (Filardy *et al.*, 2018). The literature showed that *L. major* has two putative formin genes, formin A and formin B (Chalkia *et al*., 2008). However, so far, formins from Leishmania have not been characterized. Bioinformatics data predicted that, these formins have roles in the flagellum dynamics and intraflagellar mechanism (Vasconcelos *et al*., 2008). In this report, we find the expression of *Leishmania major* formins; LmForminA and LmForminB at the RNA and protein levels. We also find the co-localization of formins, actin *in vivo* condition. Next, we pursued the role of the *L. major* formins in actin dynamics *in vitro* condition. Actin binding, bundling, and polymerization assay was carried out to inspect the effect of formin on actin dynamics. We also see SMIFH2 mediated formin inhibition has the impact of formins on *L. major* physiology.

## Experimental method

### *Parasite culture*

*L. major* Promastigotes (strain 5ASKH) were acquired from ATCC were cultured as described before (Pal et at., 2015). Cells were grown at 26°C in M199 medium (Gibco) supplemented with 15% fetal bovine serum (Gibco), 23.5 mM HEPES, 0.2 mM adenine, 150 µg/ml folic acid, 10 µg/ml hemin, 120 U/ml penicillin, 120 µg/ml streptomycin, and 60 µg/ml gentamicin.

### *Total RNA isolation and RT PCR*

Total RNA was isolated from *L. major* promastigotes using TRIzol reagent (Invitrogen) followed by DNase I (Invitrogen) digestion to remove genomic DNA contaminants using the manufacturer's protocols. cDNA was synthesized from 1 µg of total DNase treated RNA using an oligo(dT) primer and verso cDNA synthesis kit (Thermo Scientific) using the manufacturer's protocol. The

LmForminA and LmForminB FH2 domain transcripts were amplified using gene-specific primers. The primer used are same as used from LmForminA and LmForminB FH2 domain plasmid construction described below.

***Sequence alignment & Plasmid construction***

*L. major* has two predicated formins in the Protein domain prediction data-base (Chalkia *et al*., 2008). Nucleic acid sequences of predicted *L. major* formins were obtained from the database at the universal protein resource (https://www.uniprot.org/) and (https://www.ebi.ac.uk/ena/data/sequence/search). *L.major* formins FH2 domains align with the other characterized formins. Multiple sequence alignment was done using the software clustal omega (https://www.ebi.ac.uk/Tools/msa/clustalo/) and plotted using the program ESPript 3.0 (http://espript.ibcp.fr/ESPript/ESPript/) (Gouet *et al*., 1999). EMBOSS Needle, pairwise sequence alignment was also done with LmForminA FH2 domain (Accession number: Q4QE97) and LmForminB FH2 domain (Accession number: Q4QAM2).

*L.major* genomic DNA was used to amplify the gene of interest. LmForminA (695aa-1092aa) and LmForminB (714aa-1149aa) FH2 domain was cloned into the pet28a expression vector. Forward primer 5'- GGTACGGATCCGCGAGCGGCGCAGCAGCC-3' with BamH1 recognition site and reverse primer 3'-GGCCCAAGCTTTTAGCTCTGCCGCCGCTGCTTG-5' with Hind III cut site was used to amplify the FH2 domain of LmForminA. Forward primer 5'-GGTACGGATCCAAGCCGAAGCCACAGTACACC-3' with BamHI recognition site and reverse primer 5'-GAGAAGCTTCTACTGCTCCGTCGCTTCCGG-3'with Hind III cut site used for the PCR of LmForminB FH2 domain. Site-directed mutagenesis was generated by Quikchange site-directed mutagenesis protocol. LmForminA Forward primer (5'-GTGACCGAAACGTCGGCGCTGTGCTGAAGTTTATTCGGC-3'), reverse primer (5'-

GCCGAATAAACTTCAGCACAGCGCCGACGTTTCGGTCAC-3'), and LmForminB forward (5'-CAACGGTTGCAGAACATGGGCGCCGCCCTCAAGCGCGTACAG-3') reverse (5'-CTGTACGCGCTTGAGGGCGGCGCCCATGTTCTGCAACCGTTG-3') used for the mutation of isoleucine to alanine residue in FH2 domain constructs. Mutant LmForminA and LmForminB constructs were confirmed by the sequencing.

***Protein expression/purification studies***

LmForminA and LmForminB have been purified as describe in Dutta *et al* (Dutta *et al*., 2017; Harris and Higgs, 2006; Lu *et al*., 2007).

***Polyclonal Antibody generation***

Eight-week-old mice were injected with 50 µg of recombinant protein of LmForminA and LmForminB over five weeks. Seven days after the final injection, serum was collected and stored at -80ºC with 0.01% sodium azide and 10% glycerol. The generated antibody was examined against the recombinant proteins.

***Western blot with Wild-type L. major cells extract***

2 x$10^8$ log phase wild-type cells were pelleted by centrifugation at 1000g for 5 mins at 4ºC. The cells were washed with 1X PBS and centrifuged at 1000g for 5 mins at $4^0$C. The cells were then resuspended either in 100 µl of protein loading buffer (78 mM Tris-Cl pH 6.8, 0.25% SDS, 25 mM DTT. 12.5% glycerol) for LmForminA or LmForminB 100 µl of Urea lysis buffer (8 M Urea, 50 mM Tris-Cl 6.8, 25 mM DTT, 0.1 mM EDTA) mixed with an equal volume of 2X protein loading buffer and boiled for 3 minutes at 100°C with intermittent slow mixing. SDS-PAGE was immediately performed with the prepared sample. LmForminA and LmForminB were detected with raised antibodies against each protein at a primary antibody dilution of 1:1000 for both diluted in TBST buffer (10 mM Tris, 150 mM NaCl, 0.005 % (v/v) Tween20). Incubation with primary

antibody was performed overnight in cold condition with gentle shaking. The blots were then incubated with HRP-conjugated Rabbit anti-mouse secondary antibody at dilution 1:4000 for 2 hours. Finally, blots were developed using SuperSignal West Pico Chemiluminescence substrate and viewed in Syngene Chemidoc imaging system.

***Treatment of L. major cells with SMIFH2***

SMIFH2 (EMD Millipore) was freshly dissolved in dimethyl sulfoxide (100% DMSO) to prepare a 100 mM stock solution in the dark. According to the experimental requirements, further dilutions were made in DMSO before addition to the culture medium. *L.major* promastigotes were grown in a medium containing the SMIFH2 at desired concentrations for 24 hours, following which the cells were microscopically counted with a hemocytometer. Cells incubated with an equivalent concentration of DMSO (0.1%) always acted as untreated controls.

***Scanning electron microscopy of L. major cells***

The samples were prepared for electron microscopy as described elsewhere (Pal, Mondal, and Datta, 2015). Briefly, 1 $x10^7$ treated and untreated samples were taken and washed with chilled 1X PBS and centrifuged after incubation with inhibitor (in different concentration) or equivalent concentration of DMSO or PBS for 12 hours. The cells were resuspended and fixed in 200 µl 2.5% glutaraldehyde at $4^0$C for 1 hour. Cells were then pelleted and washed twice with 1X PBS, twice with Distilled water. The cells were resuspended in 200 µl of osmium tetroxide solution for 20 minutes at room temperature. Cells were again pelleted and washed with 1X PBS. The cells were gradually dehydrated by treating with a gradient of ethanol solution from 30% to 90%. Finally, cells were resuspended in absolute ethanol and spread on a cut piece of a silicon wafer, and allowed to air dry. Silicon wafer is then placed in a desiccator connected with a vacuum pump. The wafer was gold coated and viewed in Zeiss Supra 55VP scanning electron microscope. The Cell length

was quantified with ImageJ software cells being measured from cell end to end, excluding the flagella. At least 50 cells are counted for each experimental set. Unpaired t-test were performed. *P*-values ≤0.05 were considered statistically significant, and levels of statistical significance are indicated as *$P \leq 0.05$, **$P < 0.01$, ***$P < 0.001$, ****$P < 0.0001$.

***Immunofluorescence study of L. major cells***

2 x$10^6$ cells were pelleted and washed with 1X PBS and spread on poly-L-Lysine coated sterile coverslip and incubated at room temperature for 30 mins. The excess culture was removed and washed with 1X PBS and fixed with 1:1 Acetone methanol solution in the dark for 10 minutes. The cells were washed with 1X PBS and permeabilized with 0.1% Triton X 100 for 2 minutes. Cells were washed with 1X PBS and blocked with 0.2% gelatin solution for 10 minutes. Mouse anti-LmForminA (1:200), mouse anti-ForminB (1:200), rabbit anti-LmCA1 (1:200), rabbit anti-LdActin (cross-reacts with LmActin) (1:2000) was added to the coverslip and incubated for 1 hour 30 minutes. The cells were washed with 1X PBS twice and incubated with Alexa 488 goat anti-mouse and Alexa 488 goat anti-mouse antibodies for 1 hour 30 minutes. The cells were washed thrice with 1X PBS and finally mounted in anti-fade media containing DAPI. Cells were observed in Leica SP8 confocal microscope with a 63X oil immersion lens. All images are processed in LASX and ImageJ software. Image from single stack near center was presented in each case.

***Actin filament Co-sedimentation assay***

The rabbit skeletal muscle was used for the preparation of the actin acetone power. G-actin was purified from actin acetone powder with G-Buffer [5 mM Tris pH 8.0 (Sigma-Aldrich), 0.2 mM ATP (USB), 0.2 mM $CaCl_2$ (USB) and 0.2 mM DTT (USB)] (Pollard 1984). LmForminA and LmForminB protein solubility increased by dialysis in TNEG5 buffer (20 mM Tris pH 8.0, 100 mM NaCl, 1 mM EDTA, 5% Glycerol). Before dialysis, the protein was centrifuged at 14000 rpm

for 30 minutes. The Supernatant was dialyzed at 4ºC. Dialyzed protein was centrifuged again before actin co-sedimentation assay. RMA (Rabbit skeletal Actin) polymerized in TEKG5 (30 mM Tris, 1 mM EGTA, 50 mM KCl, 5% Glycerol) buffer at room temperature for 1 hour, 30 minutes. The actin polymerization was initiated by an ion mix (20X= 1M KCl, 40 mM $MgCl_2$, 10 mM ATP). Different concentrations of LmForminA and LmForminB FH2 (0.5 µM, 1 µM, 2 µM, 4 µM) were incubated with F-actin for 30 minutes. After completion of the incubation, the reaction was transferred to an ultracentrifuge tube, centrifuged at 310x1000g for 30 minutes in a TLA-100 rotor (Beckman Coulter). The Supernatant was separately mixed with 4X sample loading buffer. Pellets were resuspended in polymerization buffer to make up the volume and mixed with 4X sample loading buffer. All the samples were boiled, loaded on SDS-PAGE. Protein visualized with Coomassie (R-250) (SRL) staining (Zimmermann *et al*., 2016). An actin-bundling assay experiment similar except pre-polymerized actin was incubated with LmFormins for 30 minutes and the reaction mixture was centrifuged at 9.2 x1000g for 10 minutes at 4ºC.

The affinity of the LmForminA and LmForminB for F-actin was determined by the high-speed actin Co-sedimentation assay followed by polyacrylamide gel electrophoresis. 4µM LmForminA and LmForminB incubated with the different concentrations of F-actin (1 µM, 2 µM, 4 µM, 8 µM). The stained polyacrylamide was analyzed for densitometry using Image J software. The amount of LmForminA and LmForminB bound to F-actin was plotted vs. the concentrations of the F-actin. The dissociation constant ($K_D$) of LmForminA and LmForminB was determined by non-linear curve fitting.

***Surface Plasmon Resonance***

Interaction of actin with *L. major* formins was corroborated by the surface Plasmon resonance technique (SPR) using a Biacore T200 system. Biacore Series S Sensor Chip NTA (consists of

carboxymethylated dextran with covalently immobilized NTA) was utilized to capture LmForminA and LmForminB (ligand). 0.5 mM NiCl used for the binding of the poly-Histidine tags LmForminA and LmForminB. G-buffer used as a running buffer. Different concentrations of F-actin (0.5 µM, 1 µM, 2 µM, 4 µM) flown onto the capture LmForminA and LmForminB in running buffer. The LmForminA and LmForminB interaction with F-actin was monitored by an increment in the response units. Surface regeneration was conduct by introducing 800 mM imidazole for 60 seconds. Double referencing (blank of the surface without a ligand and buffer injections) was also performed to eradicate the chance of nonspecific interaction.

***Actin nucleation assay by fluorescence spectroscopy***

Unlabeled and pyrene labelled actin were mixed (10% labeled final) with G-buffer to produce 12 µM actin stock (RMA). The polymerization reaction was prepared with the 2 µM RMA in the presence of $MgCl_2$ and EGTA. The Polymerization reaction's remaining volume makes up with the HEKG5 buffer, and different concentrations of *L. major* formins were added. Actin polymerization was initiated by adding the 20X Ion-mixed (40 mM $MgCl_2$, 10 mM ATP, 1 M KCL) buffer. Actin polymerization was observed by the N-(1-pyrene) iodoacetamide (P-29, Molecular Probes) labelled rabbit muscle actin (RMA) for the direct observation of fluorescence at 25ºC (Higgs and Pollard, 1999; Moseley *et al*., 2006). The fluorescence of pyrene actin excitation (365 nm) and emission (407 nm) wavelength was monitored by fluorescence spectrophotometer (QM40, Photon Technology International, Lawrenceville, NJ) (Moseley *et al*., 2006). Actin assembly rates were determined by the slopes of fluorescence curves at 50 % actin polymerization (Moseley and Goode, 2005).

***Barbed end elongation by Fluorescence Spectroscopy***

10 µM unlabeled actin was polymerized in F-buffer for 4 hours at room temperature. F-actin was sheared by passing through the 27-gauge needle for five times used as actin seed. F-buffer, along with the LmForminA and LmForminB were added to the actin seed and mixed gently. G-actin (10% pyrene-labelled) was added to actin seed with cut tips, mixed twice by pipetting up-down and final reaction placed in the fluorometer cuvette. The fluorescence was measured at 365/407nm and record for 1000 seconds (Moseley *et al*., 2006). Elongation rate was determined by the linear fitting of the initial 100 seconds elongation (Christensen *et al*., 2019).

In barbed end capping experiment capping protein and *L. major* formins were added simultaneously to the F-actin seed, then added to the actin monomers and monitor the fluorescence of the actin filament elongation.

***TIRF Microscopy***

G-actin was polymerized to F-actin in polymerization buffer (10 mM Tris-Cl pH 8.0, 0.2 mM DTT, 0.2 mM ATP, 0.2 mM $CaCl_2$) for 1 h at room temperature. 500 nM LmForminA and LmForminB added on the 2.5 µM actin filaments mixed gently. Polymerization buffer, Alexa-488-phalloidin add and reaction diluted in imaging buffer [20 mM HEPES (USB), 1 mM EDTA (Sigma), 50 mM KCl (Sigma-Aldrich), and 5% Glycerol] immediately. Samples were applied on the poly-D-lysine coated 22 mm coverslip. Samples were imaged by the Olympus TIRF IX83 microscopy using 100×1.49 N.A. objective.

0.5 µM actin was polymerized in the presence of the LmForminA and LmForminB for the observation of the actin nucleation activity. The time-lapse image capture after 10 seconds interval for 10 minutes. The number of filaments quantified over time frames by using the Image J software.

**Results**

### *Leishmania major possesses two formins*

Bioinformatics analysis of *L.major* genome predicts the presence of two putative formins LmForminA and LmForminB, in chromosomes; chromosome 17 and chromosome 24 (fig. 1A) (Ivens, 2005). Total RNA was extracted, DNase treated, and cDNA synthesized from it was used as the template for PCR with FH2 domain specific primers for both the formins. 1191 bp and 1305 bp bands were observed for LmForminA and LmForminB, respectively, indicating expression at RNA level (fig. 1B). Western blot with a specific antibody raised against the FH2 domain of LmForminA, for *L. major* whole cell lysate shows a distinct band of ~180 kDa and some bands in between 100-135 kDa, which is higher than the predicted molecular weight of the protein (138.38 kDa). A higher than expected molecular weight of LmForminA might be due to post-translational modifications (fig. 1C). Similarly, western blot with LmForminB specific antibody raised against the FH2 domain indicates a single band at 129.19 kDa as expected (fig. 1D). Taken together, our data confirmed that *L. major* cells constitutively express two formins, LmForminA and LmForminB.

### ***Both LmForminA and LmForminB has patchy localization***

Next, we asked the question where these formins are localized within the parasite. Immunofluorescence study with LmForminA antibody shown patchy distribution with a prominent punctum near the nucleus and kinetoplast (Fig 2D). LmForminB also shows a patchy distributed pattern inside the cell. LmForminA puncta partially colocalize with *L. major* Carbonic anhydrase, a cytosolic marker (Pal et at., 2017), indicating the puncta is cytosolic (fig. 2D). Additionally, the LmForminA puncta also colocalize with the actin patches, i.e., it might be bound with the actin inside the cell, thus giving it the distinctly distributed localization (fig. S1).

Similarly, LmForminB puncta also colocalize with LmCA1 partially and with LmActin with in the cell.

***Growth of Leishmania major cells are inhibited by formin inhibitor SMIFH2***

To check the physiological importance of formins, *L. major* promastigotes were grown in the presence of an increasing concentration of SMIFH2, a formin FH2 domain inhibitor (Rizvi *et al*., 2009), which showed a dose-dependent decrease in cell number with $IC_{50}$ value determined to be 11.86 µM (fig. 2B). Scanning electron microscopy of the SMIFH2-treated *L.major* cells shows a morphological abnormality, where cells become shortened with rounded shape in the presence of the inhibitor (fig. 2A, C ). The length of the parasite is significantly reduced at even at 2.5 µM concentration of inhibition, which is more than one-fourth of the $IC_{50}$ (11.86 µM), which might indicate the rounding and reduction of cell length is not due to general stress, but due to affect in the cytoskeleton dynamic of the pathogen. In other word, formins seem to play an important role in maintaining cell shape and morphology. DMSO itself does not affect growth or morphological changes as observed with DMSO control (fig. 2A, B and C).

***Purified Leishmania major formins can bind F-actin***

As both the formin had been colocalized with actin inside *L.major* cells (fig. S1), we next attempted to clone and purify LmForminA and LmForminB FH2 domain to test their interaction with F-actin (fig. S4A). LmForminA and LmForminB FH2 domains were purified as N-terminal 6 His-tag protein (fig. S4B). Co-sedimentation assay with LmFormins FH2 domain and actin filaments showed that LmFormins were precipitate in the pellet fraction along with actin. However, in control experiments without actin, LmForminA and LmForminB proteins remained in the supernatant fraction (fig. 3A, B, respectively). Results indicate that LmForminA and

LmForminB protein have an F-actin binding ability in the *in vitro* condition with the FH2 domain similar to other well-characterized formins (Shimada *et al*., 2004; Dutta *et al*., 2017).

The dissociation constant of LmForminA and LmForminB binds with F-actin actin were determined by analyzing the SDS-PAGE gel of co-sedimentation assay. The fraction of bound LmFormins with F-actin curve fitting shows the $K_D$ value 1.84 µM and 0.2 µM for LmForminA and LmForminB, respectively (fig. S5C, D). This dissociation constant value indicated that LmForminB has a greater affinity than LmForminA. To reconfirm the LmFormins interaction with F-actin, we had used surface plasmon resonance. In this experiment, LmForminA and LmForminB were used as capture ligand and F-actin as analyte. Different concentrations (0.5µM, 1µM, 2µM, 4µM) of shared F-actin filaments were used to see the interaction with LmForminA and LmForminB. Interaction of LmForminA and LmForminB with F-actin was monitored by an increase in response to different ligand which ligand concentrations (fig. 3C, D).

***Leishmania major formins could form an actin filament bundled***

Literature has depicted that some formin has side binding with actin filament leads to the formation of an actin filament bundle (Harris, Li and Higgs, 2004; Michelot *et al.,* 2005). In Bnr1p and Daam1 C-terminal domain, which have FH1, FH2, and C-terminal end, are responsible for actin filament bundling (Moseley and Goode, 2005; Barkó *et al*., 2010). In Arabidopsis formin AFH1, the FH1 domain is also required along with the FH2 domain for actin-bundling (Michelot *et al*., 2005). While mDia2, FRL1 formin only FH2 domain is a strong actin filament bundler (Harris *et al*., 2006). F-actin bundling activity of formin might have very important for the physiology of the organism. However, till now, no actin-bundling activity had been shown for the formin from the protozoan Kinetoplastida group. *L. major* contains a short F-actin bundle in the cell (Sahasrabuddhe, Bajpai, and Gupta, 2004). We were interested to know that LmForminA and

LmForminB have any role in F-actin bundling. Actin-bundling ability of purified LmForminA and LmForminB was determined by co-sedimentation assay at low-speed centrifugation. Polymerized Filamentous actin at low-speed centrifugation remained in the supernatant fraction. In the presence of the LmForminA and LmForminB, F-actin co-sedimented in the pellet fraction at low-speed centrifugation that indicates actin filament bundling activity (fig. 5A, B). Fascin was used as a positive control, a well-characterized actin-bundling protein that also brings the F-actin in pellet fraction at low-speed co-sedimentation assay (fig. S5E) (Yamashiro *et al*., 1998).

We used a TIRF microscope to examined the F-actin bundle formation by LmForminA and LmForminB. Pre-polymerized actin filaments were incubated with the LmFormins and stained with the phalloidin, and observed in microscopy. We found a long thick actin bundle in the presence of the LmForminA and LmForminB (fig. 5C). LmFormins induced thick actin filament bundles were quantified by measuring the thickness of the filaments. The width of the single filament compared with the thick bundled filaments. The F-actin bundled width is 2-3 times more as compared to the actin control indicated that LmForminA and LmForminB have actin-bundling ability *In vitro* conditions. More numbers of actin filament bundles were found in the presence of the LmForminA as compared to LmForminB. Results indicated that LmForminA has a strong actin-bundling activity, while LmForminB has a weak actin-bundling activity.

The electrostatic interaction between the FRL1 and mDia2 FH2 domain and actin is important for their bundling activity. Salt ionic strength affects the mDia2 and FRL1 FH2 domain actin-bundling activity (Harris *et al*., 2006). We also tested whether LmForminA and LmForminB FH2 domain actin-bundling affected by the ionic strength condition like mDia2 and FRL. We find increasing the ionic concentration of KCL (50 mM, 100 mM, 150 mM) affecting the actin pelleting efficiency of the LmForminA. LmForminA actin pelleting efficiency reduced at 100 mM concentration of

KCl and almost lost at 150 nM KCl concentration (fig. S7A). Whereas LmForminB actin bundling activity was slightly affected with a high concentration of KCl (fig. S7B).

***Leishmania major formins increase actin polymerization***

Most characterized Formin FH2 domain shows strong activity in terms of nucleation of actin filaments in *in vitro* condition, expects FHOD1 FH2 inhibits the polymerization of the actin filament (Schonichen *et al*., 2013). Actin polymerization by the formin FH2 domain is also reported in human parasites like *Plasmodium falciparum, Toxoplasma gondii*, where formin plays some important role in their physiological function. *Plasmodium falciparum* used actin-based motility to invade the host cell, which is achieved by PfFormins. It has been shown that PfFormin1 and PfFormin2 able to polymerize chicken muscle actin *in vitro* conditions (Baum *et al*., 2008).

We had explores the actin nucleation activity of *L.major* formins by spontaneous actin assembly by pyrene actin fluorometric assay. 2µM Actin control shows polymerization at a basal level, while the LmForminA and LmForminB effectively increased actin polymerization in a concentration-dependent manner (fig. 4A, C). The comparative analysis demonstrated that LmForminB has a higher rate of actin polymerization than LmForminA (fig. 4B, D).

Total internal reflection fluorescence microscopes were executed to study the direct visualization of actin filament polymerization activity in the presence of the LmForminA and LmForminB. Actin was polymerized in the presence and absence of LmForminA and LmForminB and analyzed in TIRFM. More actin filaments were observed in LmForminA and LmForminB than actin control (fig. 4E).

***Leishmania major inhibits elongation and antagonizes the capping protein***

Literature has shown that the barbed end of actin filaments captured by formin affects the barbed end elongation. Formins accelerate barbed end elongation of actin filaments in the presence of the

393 profilin and decrease barbed end elongation in the absence of profilin (Patel *et al*., 2018). We
394 performed a barbed end elongation assay to test the effect of the LmForminA and LmForminB on
395 actin filaments elongation.
396 We found that LmForminA and LmForminB have no effect on barbed end elongation in the
397 presence of the lower concentration (100 nM) LmFormins. In contrast, at higher concentrations,
398 LmForminA and LmForminB show decreased actin filaments elongation compare to actin control
399 (fig. 6A, B). LmForminA and LmForminB inhibit the filament elongation ~63% and ~35% at 1µM
400 concentration. This attribute effect might be due to the actin bundle formation by LmForminA.
401 LmForminA induced actin bundle formation leads to shortage of free barbed end of the actin
402 filament. So, filament's free end is not accessible for the addition of actin subunits on the barbed
403 end. LmForminB, a weak actin bundler, has the more free filaments end for the actin filament
404 formation.
405 Next, we performed TIRF microscopy to see the effect of LmForminA on filament elongation. 500
406 nM LmForminA incubated with the actin filaments. Where actin bundled was appeared in the
407 presence of LmForminA (Data not shown). Based on the observation, we speculate that the actin
408 elongation rate was decreased due to the actin bundle formation in the presence of the LmForminA.
409 Formin FH2 domain has a processive activity for filament barbed end. Literature shows mDia1,
410 FRL, and Bni1 protect the barbed ends from the capping proteins (Harris, Li and Higgs, 2004;
411 Harris *et al*., 2006). We were interested in seeing that LmForminA and LmForminB will be able
412 to protect the barbed end from the capping protein. Capping protein binds with the barbed end and
413 inhibits the actin filament elongation. Here we mixed LmFormins and capping protein
414 simultaneously with the actin filament seed and then added actin monomer to initiate the
415 elongation. In the presence of the capping protein, LmFormins allows the actin filaments

elongation (fig. 6E, F). Based on the result, we speculate LmFormins not only processively binds with the barbed end and activity replacing the capping protein but might also be competing for the barbed with the capping protein.

***(I-A) mutant of LmForminA and LmForminB can bind actin and bundle actin filament***

Isoleucine and lysine are the highly conserved amino-acid residues in the formin FH2 domain. These residues are crucial for actin assembly in most of the reported formins (Harris *et al*., 2006; Scott, Neidt and Kovar, 2011). In Bni1 and Daam1, mutations of isoleucine to alanine altogether abolish assembly activity (Lu *et al*., 2007; Xu *et al*., 2004)**.** Based on the sequence alignment of LmForminA and LmForminB with other characterized formins (fig. S2), we also find the conserved isoleucine residues in LmForminA and LmForminB. We generate a point mutation for conserved isoleucine to alanine in LmForminA and LmForminB FH2 domain at specific position (fig. S2). Interaction of mutant LmFormins with F-actin was confirmed by the surface plasmon resonance (fig. S4C, D). We had measured the actin nucleation activity of the mutant LmFormins by the pyrene actin assembly assay. We found that the I777A LmForminA has significantly less actin nucleation activity (fig. 7A). I802A LmForminB has shown a mild effect on actin assembly (fig. 7C). Actin assembly reduced 2~3 fold in the I802A LmForminB as compared to wild-type LmForminB (fig. 6D). We conclude that the conserved isoleucine residue is crucial for actin assembly in LmForminA as compared to LmForminB.

Mutation in conserved amino acid residues Ile to ala in frl1, mDia2 did not affect the actin-bundling activity (Harris *et al*., 2006). In LmFormins, the influence of (I-A) mutation on the actin-bundling activity was observed by a co-sedimentation assay. The Low-speed co-sedimentation assay shows the actin pelleting activity in the presence of I777A LmForminA and I802A LmForminB (fig. S4F, G). The actin pelleting activity of I777A LmForminA is similar to wild-

type LmForminA. I802A LmForminB actin-bundling activity slightly increased as compared to wild-type ForminB. Similar results were obtained when wild-type and I777A LmForminA constructs incubate in the reaction before actin polymerization. Wild-type LmForminB unable to actin bundle formation in case of co-polymerization, while LmForminA actin-bundling activity does not affect. Based on the observation, we speculate that (I-A) mutation might have increased the side bundling activity of actin in LmForminB, while it does not affect LmForminA.

We also performed a barbed end elongation assay to understand the effect of mutant LmFormins binding with the barbed end and protecting from capping protein. Mutant LmFormins binding with the barbed end has no significant influence on actin filaments elongation as compare to wild-type LmFormins. The addition of Capping protein on actin filaments in the presence of the Mutant LmFormins have significantly reduced the ability to protect the barbed end from capping protein in comparison to the wild-type LmFormins (fig. S6A, B). This result indicates that mutant LmFormins might have dissociated fast from the barbed end than wild-type LmFormins providing accessibility for capping protein binding.

**Discussions**

Formins are essential proteins involved in a range of cellular functions from cell division to trafficking (Castrillon and Wasserman, 1994; Evangelista *et al.*, 2002; Maas *et al.*, 1990; Sagot, Klee and Pellman, 2002). Recently, formins from parasitic protozoans such as *Plasmodium, Toxoplasma* have been shown to be very important for infectivity (Baum *et al*., 2008; Daher *et al*., 2010; Daher *et al*., 2012; Tosetti *et al*., 2019; Dippe, von Dippe, and Levy, 1982; McConville *et al.*, 2002; Stortz *et al.*, 2019). Nevertheless, nothing was reported in the case of the Kinetoplasts *Leishmania,* although the importance of actin and other actin-binding proteins such as Arp2/3 complex, cofilin, profilin are well reported (Ambaru *et al*., 2020; Tammana *et al*., 2010). This

462 class of distinguished actin-binding proteins formin plays a curious role in a eukaryotic organism,
463 including a parasite group but it is still not functionally characterized in *Leishmania*.
464 To uncover the functional aspect of formin, we first treated *L. major* cell with SMIFH2 (Formin
465 inhibitor). Our data indicate that formin inhibitor SMIFH2 affects *L. major* cell growth. Growth
466 inhibition was observed with SMIFH2, with $IC_{50}$ being 11.86 μM, which is comparable to other
467 reports such as in fibroblast cells where cytotoxicity was observed at 28 μM in mammalian cells
468 (Rizvi *et al*., 2009), 40 μM in Epithelial ovarian cancer cells (Ziske et al., 2016). In addition to
469 that, cells appeared rounded, in concentration as low as 2.5 μM of SMIFH2; this might indicate,
470 the rounding of the cell is due to perturbation of cytoskeleton dynamics rather than general stress.
471 It confirms the importance of active formin in *L.major* physiology, which might be crucial for
472 *Leishmania* survival. *Searching* in the genome database, we found two putative formins, namely
473 LmForminA and LmForminB (Ivens *et al.*, 2005). We observed LmFormins expression at the
474 RNA and protein levels (fig. 1A). Bands at western blot were observed in the case of protein at
475 higher molecular weight than predicted, indicating there might be a post-translation modification
476 (fig. 1C) similar observation has been recorded in the case of DAAM1, FMNL2 in mammalian
477 cells (Li *et al.*, 2019). The most characterized formins use RhoA mediated regulation to regulate
478 their activity. However, the literature and genome database has not shown the presence of RhoA-
479 GTPase gene in *Leishmania*, which could have been necessary to regulate the formin activity in
480 leishmania. A related RhoA-GTPase gene is present in *Trypanosoma* but is absent in *L. major*
481 (Abbasi *et al.*, 2011). The absence of the Rho-GTPase suggests that *L.major* formins activity
482 regulation used a distinct approach from the mammalian system. As a result, it indicates the post-
483 translation modification in LmFormins, which might play an important role in regulating formins
484 activity in *L.major* (DeWard and Alberts, 2009; Angeles Juanes and Piatti, 2016). The post-

translational modification is a well-characterized phenomenon observed in *Leishmania* (Zilberstein, 2015).

Next, we were interested to see how these LmFormins regulate the actin dynamics *in vivo*. To see its effect on actin dynamics first, we have to determine where these formins localized in the cell: For these localization studies, we had raised LmForminA and LmForminB specific antibody. LmForminA and LmForminB did not possess any predicted signal peptide for the secretory pathway or mitochondrial specific suggested that both the formins are localized in the cytosol. Our research group's previously studied LmCA (*L.major* carbonic anhydrase) localized in the cytosol is used as a positive control for conforming to the localization data (Pal *et al.,* 2017). LmFormins localization patches are similar to other cytoskeleton binding proteins' pattern such as myosin, coronin (Drubin, Miller, and Botstein, 1988; Sahasrabuddhe, Nayak, and Gupta, 2009). LmFormins patches are colocalized with *L.major* actin indicate that LmFormins binds with the actin cytoskeleton inside *L. major* cell (fig. S1).

Next, we were interested to see how LmFormins regulates actin dynamics *in vitro* conditions. FH2 domain is the characteristic feature of the formin family, which is the crucial player for the formin activity in regulating the actin dynamics. *L.major* putative formin genes have one FH1 and FH2 domain (Chalkia *et al*., 2008). *L.major* Formins FH2 domain sequence aligned with well-characterized formins shown the conserved amino acid with identity around 20.1%-40.9%. Pairwise alignment Results reveal that LmForminA has 57% similarity with *Trypanosoma cruzi* ForminA. The characterized formin of *Dictyostelium discoideum has* 44% similarity with LmForminA and 39% similarity with LmForminB (fig. S2).

Our study reveals that LmForminA and LmForminB FH2 domain can interact with actin *in vitro* conditions. LmFormin-FH2 domain binds with F-actin in a concentration-dependent manner. The

binding affinity of LmForminB shows a strong affinity with a lower $K_D$ value (0.2 µM) as compared to the LmForminA ($K_D$=1.84 µM). Lower dissociation constant of LmForminB showing comparable less affinity than to the FRLα and FRLβ (Harris et al., 2004). But higher affinity than the mDia1, mDia3, and Bni1(2-7µM) (Harris, Li, and Higgs, 2004; Li and Higgs, 2003; Shimada *et al.*, 2004).

LmForminA and LmForminB also have a feature to bundle actin filaments *in vitro* condition. The low-speed co-sedimentation assay is indicating the LmFormins has actin-bundling properties. Microscopic observation of F-actin in the presence of the LmForminA and LmForminB has confirmed their actin-bundling feature. Earlier reports already describe some formins having actin filaments bundling activity. These actin-bundling formins are budding yeast Bnr1p (Moseley and Goode, 2005), *Dictyostelium* ForC (Junemann *et al*., 2013), mammalian FRL1, and mDia2 (Harris *et al*., 2006), *Arabidopsis* AFH1 (Michelot *et al*., 2005), *Drosophila* FHOD1 and FHOD3 (Patel *et al*. 2018) and *Drosophila* Daam1 (Barkó *et al*. 2010). Most recently reported mice delphilin is a weak actin bundler (Silkworth *et al*., 2018). According to the literature, in the protozoan parasite group, only *Toxoplasma gondii* formins have actin-bundling activity (Skillman *et al*., 2012). The above-characterized actin-bundling formins have a common feature: they possess positively charged amino acids in FH2 domains with higher PI value. LmForminA FH2 domain used in this study has a PI value of 8.31, which is higher than the mDia1 and Bni1 (PI value 6.37 and 5.64, respectively) could not form an actin bundle. FRL1 and mDia2 (PI value 8.26 and 8.14, respectively) can firmly form an actin bundle. PI value of LmForminA 8.31 is close to the PI value of mDia2 and FRL1 (Harris *et al*., 2006). LmForminB, a weak actin bundler, has a PI value of 7.09, which is higher than the PI value of 5.89 for Delphilin, also a weak actin bundler (Silkworth *et al*.,2018). As an earlier hypothesis, the net positively charged amino-acid of the FH2 domain

involved in the actin bundle formation while the net negativity charge FH2 domain could not form actin bundle (Harris *et al*.,2006). The bundling activity difference in formins indicates that the positively charged amino-acids of the FH2 domain might mediate the electrostatic interaction with the negatively charged actin filament residues for actin bundling. We find, this presumption is strongly supported by the salt susceptivity of LmFormins bundling activity, which might reduce the electrostatic interaction are significant for actin-bundling activity. mDia1 (PI value 6.37) net negatively charged amino-acids at the outer surface would not form an actin bundle (Harris et al., 2006). In the absence of the crystal structure of the LmForminA and LmForminB, we could not describe the outer surface amino-acids, but the LmForminB PI value slightly higher than the mDia1 supports this kind of assumption (Harris *et al*., 2006).

*L. major* actin present in the patches (Sahasrabuddhe, Bajpai, and Gupta, 2004). It has been reported that coronin protein is vital for actin-bundling in *Leishmania* (Nayak *et al*., 2005). Actin bundled structure formation in Leishmania might not be solely coronin dependent. Formins might be playing a pivotal role in actin bundle formation inside the *Leishmania* cell. What are the physiological effects of this actin bundle in *Leishmania* is not still clear. LmForminA and LmForminB actin bundling activity differences might point to their different phenotype, localization, and regulation. *In vitro* biochemical assay based on the pyrene labelled actin assembly shows that LmFormins increase the actin polymerization concentration-dependent manner. LmForminB is a more potent actin nucleator as compare to LmForminA. The intense nucleation activity of LmForminB as compare to LmForminA might have some physiological significance *in vivo.*

In the actin assembly rate comparison, LmForminA with mammalian Formin Daam1 exhibits a similar polymerization rate. While LmForminB has a four-fold higher polymerization rate. The

554 important role of the actin polymerization in the presence of the formins has already been reported
555 in some protozoan parasites. In *Toxoplasma gondii* formin, TgFRM1, TgFRM2 & TgFRM3 is also
556 a potent actin nucleator *in vitro* condition. TgFRM1 and TgFRM2 formin play an essential role in
557 parasite mobility and host cell invasion (Daher *et al*., 2010). The malaria parasite *Plasmodium*
558 *falciparum* invade host cell by using actin-based motility, which shows that formin is important in
559 actin polymerization involved in the motility (Baum *et al*., 2008).Structural analysis of the Bni1p
560 and mDia1 has shown that conserved amino-acid Ile residue faces the inside of the FH2
561 homodimer, this residue of the FH2 domain creates important interaction with the actin molecule
562 (Xu *et al*., 2004). Moreover, a mutation in this residue completely abolishes actin assembly.
563 Investigating the point mutation (Ile-ala) in LmFormins, we found it has a different effect on actin
564 assembly. This mutation completely abolishes the actin assembly of LmForminA, similarly Daam1
565 and *Drosophila* Fhod (Barkó *et al*., 2010; Xu *et al*., 2004). Mutant LmForminB has a mild effect
566 on actin assembly. The Ile-ala mutant of FRL1 also has a mild effect on the actin assembly (Harris
567 *et al*., 2006).
568 (I-A) mutation might affect the flexibility of the FH2 domain and might suppress the switch from
569 the closed to the open configuration during actin assembly. To understand the actual mechanism,
570 the resolution of the FH2 domain structure of LmForminA and LmForminB in the presence of the
571 actin would be necessary.
572 In barbed end elongation assay, we find LmFormins did not accelerate the barbed end elongation.
573 It was not an unexpected result because some formin such as Drosophila Fhod, Drosophila Daam1,
574 and mice FRLα also share this classical characteristic of the barbed end elongation (Barkó *et al*.,
575 2010; Patel *et al*. 2018; Harris, Li, and Higgs, 2004). LmFormins reduced the barbed end
576 elongation in the absence of the profilin like the Drosophila Fhod. LmFormins slows the barbed

end elongation due to its binding of the FH2 domain that spends most of the time in a closed conformation similar to *Drosophila* Fhod (Barkó *et al*., 2010). LmFormins binds to the barbed and protects from the capping protein. LmFormins barbed end binding and antagonizing the capping protein nature Indicates that (1) LmFormins and capping protein might passively compete for the barbed end binding on elongating filaments. (2) LmFormins form a processive cap that maintains an association with the barbed end during filament elongation and replacing the capping protein from the barbed end. Compared to wild-type LmFormins, mutants have similar actin elongation activity but have significantly less barbed end protecting activity from the capping protein. Similarly, Ile to ala mutation in Drosophila Fhod, FRL1, and mDia1FH2 also decrease the barbed end elongation (Barkó *et al*., 2010; Harris *et al*., 2006).

Our study shows the biochemical properties of the LmFormins FH2 domain and its effects on the actin dynamics. LmFormins FH2 domain overall features are similar to the other Formins. However, it is still unclear what are the exact role of LmFormins in *Leishmania* physiology. Some other important domains, such as RBD, DAD, DID are not predicted in the case of LmFormins. Together, this indicates, there are most probably differences in regulation of formins in *Leishmania* compare to mammalian counterpart. Exploration of such might lead to new therapeutics against the vicious parasite.

**Acknowledgements:**

The authors sincerely thank Mr. Kashinath Sahu for their expert technical assistance in SEM imaging and Jajati Keshari Ray for mice handling. The authors also thank Dr. Amogh Sahasrabuddhe for providing the LdActin antibody. The authors also thank Dr. Arnab Gupta, Ruturaj and DBT Welcome imaging facility, IISER Kolkata for helping with confocal microscopy. The authors also thank Dr. Bidisha Sinha for providing TIRF microscopy for imaging and Rinku

Kumar Patel, Madhura Chakraborty and Arikta Biswas for their assistance in TIRF microscopy imaging.

**Competing interests:**

The authors declare that they do not have any conflict of interests.

**Author contributions:**

Conceived and designed the experiments: SM RD. Performed the experiments: RK AS JAS RPB DD. Analyzed the data: SM RD. Wrote the manuscript: SM RD RK AS JAS.

**Funding:**

R.K. was supported by an individual fellowship from the University Grant Commission and A.S. was supported by an individual fellowship from the Council of Scientific and Industrial Research, Government of India. The work was supported by Department of Biotechnology funding number BT/PR26167/MED/29/1229/2017

**FIGURE LEGENDS**

**Figure 1. Expression of the two Formins in *Leishmania major.***

[A] Schematics diagram showing the organization of the predicated FH2 domain of LmForminA and LmForminB. The LmFormins constructs used in this work span residue is LmForminA(695-1092aa) and LmForminB (714-1149aa) with predicted PCR products of 1191 bp and 1305 bp. [B] Expression analysis of LmForminA and LmForminB by RT-PCR. The lanes marked –RT represents negative control with the RT enzyme. Bands of 1191 bp and 1305 bp observed in LmForminA and LmForminB FH2 domain PCR respectively. [C] Western blot with anti-Formin A and anti-Formin B antibodies with *L. major* whole cell lysate.

**Figure 2. SMIFH2 affects the growth of *Leishmania major* Growth.**

[A] Scanning electron micrographs of SMIFH2 treated and untreated *L. major* cells. Cells were treated 12 hours with/without SMIFH2 in respective concentrations. Images were acquired Zeiss Supra 55VP scanning electron microscope. [B] Cell lengths were quantified using ImageJ software. Asterisks indicate a significant difference between untreated with respect to treated cells. ***P*<01 *****P*<0.0001 (Student's *t*-test). [C] Growth kinetics of *L. major* cells in the presence of formin inhibitor SMIFH2 grown for 24 hours. The cell number was normalized with respect to DMSO control. Error bar represents the standard deviation from 3 independent experiments. [D] Confocal imaging of *L. major* cells immunostained with DAPI (blue), anti-Formin A, and anti-Formin B (green) (1:200) anti-LmCA1 (cytosolic marker) (red) (1:200), acquired in LeicaSP8 confocal microscope. Partial colocalization (yellow) was observed in both cases. Scale bar represents 10 µm.

**Figure 3. *L.major* ForminA and ForminB bind with F-actin *invitro* conditions.**

[A, B] 10% Coomassie-stained SDS-PAGE of LmForminA and LmForminB binds to F-actin. LmForminA and LmForminB incubated with F-actin for actin binding. Co-sediment at high-speed centrifugation for analyzed the LmForminA and LmForminB binding. LmForminA and LmForminB actin control most of the protein that remains in the supernatant fraction, while actin controls most of the fraction that remains in the pellet. LmForminA and LmForminB, which bind with the actin present in the pellet, indicated binding with F-actin. [C, D] Surface Plasmon resonance was performed to see the interaction of LmForminA and LmForminB with F-actin. LmForminA and LmForminB capture on an NTA chip and different concentrations of F-actin (0.5, 1, 2, 4 µM) flowed on capture LmForminA and LmForminB. The Sensorgram has shown the

643 interaction phase of LmForminA [C] and LmForminB [D], followed by the dissociation phase.
644 The interaction has been seen by an increase in response in a concentration-dependent manner.

645 **Figure 4. *L.major* ForminA and ForminB efficiently accelerate an actin assembly *in vitro***
646 **condition.**

647 [A, B] 2 µM rabbit muscle actin (10% pyrene-labeled) used for actin assembly. Data (A, B) shows
648 actin assembly in the presence or absence of LmForminA and LmForminB respectively. Actin
649 assembly increased in a concentration-dependent manner in the presence of the LmForminA and
650 LmForminB. [C, D] Data (A, B) was used for the quantification of actin assembly rate at half-
651 maximal polymerization of actin in the presence of a different concentration of LmForminA and
652 LmForminB. A.U., arbitrary units. [E] 0.5 µM Actin used for polymerization in the presence or
653 absence of 25 nM LmForminA and 10 nM LmForminB, respectively. Alexa-488-phalloidin is used
654 for the staining of actin. The image was captured by TIRF microscopy. A time-lapse image has
655 captured shows an increase in the number of filaments in the presence of the LmForminA and
656 LmForminB as compared to actin control. Scale bar 10 µM.

657 **Figure 5. *L.major* Formin A and Formin B formed F-actin bundled *in vitro* conditions.**

658 [A, B] 10%Coomassie-stained SDS-PAGE of LmForminA (A) and LmForminB (B) to verify the
659 F-actin bundling. F-actin incubate with LmFormins and Co-sediment at low-speed centrifuge.
660 Actin bundled coming in pellet fraction in the presence of the LmForminA and LmForminB,
661 indicating formin bundling nature**.** [C] TIRF Microscopic image for direct visualization of the
662 event in actin-bundling in the presence of the 500 nM LmForminA and 500 nM LmForminB.
663 LmForminA and LmForminB protein mixed with 2.5 µM polymerized Actin filaments stained
664 with Alexa-488-phalloidin. 20 µl diluted reaction taken inflow chamber imaged capture by the

TIRF Microscope. Thick filaments bundled were capture in the presence of the formin. The scale bar is 10 µM. Actin-bundling fascin served as a positive control.

**Figure 6. *L.major* Formins inhibits actin elongation and antagonizes capping protein.**

[A, B] Actin elongation performed in the presence of the preformed actin seed. Preformed actin seed was prepared by F-actin passing from the 27 gauge needle five times. Actin seed mixed with (10%) pyrene labelled G-actin. Actin elongation was performed in the presence and absence of different concentrations of LmForminA and LmForminB. Actin elongation decrease in the presence of LmForminA and LmForminB in a concentration-dependent manner. [C, D] Elongation rate quantification from (A, B) measured as the initial slope over the first 100 seconds. [E, F] 0.5 µM G-actin (10% pyrene-labelled) with F-actin seed used in actin elongation with various concentrations of LmForminA and LmForminB. LmForminA and LmForminB mixed before the capping protein to see the LmFormins antagonize to capping protein. Actin elongated in the presence of LmFormins, antagonizing the capping protein from the barbed ends.

**Figure 7. *L.major* Formins nucleation efficiency is affected by I-A mutation.**

[A] Direct comparison of actin assembly in the presence of the wild-type and mutant I777A LmForminA. Actin assembly severely affected in mutantI777A LmForminA. [B] Actin polymerization in the presence of the wild-type LmForminB and mutantI802A LmForminB. Mutation in conserved amino acid residues I802A has shown a mild effect on actin assembly. [C, D] Actin polymerization rate quantification from (A, B) respectively.

**Supplementary Figure**

**Figure S1. LmFormins co-localized with the actin *in vivo* condition.**

Confocal imaging of L. major cells immunostained with DAPI (blue), Anti-Formin A, and Anti-Formin B (green) (1:200) LdActin (cross-reacts with LmActin) (red) (1:2000), acquired in

LeicaSP8 confocal microscope. Partial colocalization (yellow) was observed in both cases indicated with white arrows. Scale bar represents 10 µm.

**Figure S2. LmFormins has a conserved amino-acids similar to the other characterized formins.**

Multiple alignments of the amino-acid sequence of the FH2 domain of the LmForminA and LmForminB from different organisms. *L. major* putative formin A (Q4QE97) and formin B (Q4QAM2) amino acid sequence compared to the characterized formin FH2 domain from human Daaam1(Q944D1), mouseDia1 (o08808), *Dictyostelium discoideum* (Q54N00), *Arabidopsis thaliana* (Q9SE97), *Saccharomyces cerevisiae* (P41832, P40450), *Trypanosoma cruzi* (Q4D1V1). Strictly conserved residues are shown in the black box, identical residues are boxed in red. While sites showing the similarities are shown in a blue box. Dashes indicate gaps introduced for optimal alignment

**Figure S3**. **Pairwise alignment shows LmFormins has some identical amino-acids as other eukaryotic organisms.**

LmForminA and LmForminB Pairwise alignment data with different formins are shown in the table.

**Figure S4. Ile-Ala Mutant LmForminA and LmForminB interact with the F-actin and can still form actin bundle.**

**[A]** Purified plasmids of LmForminA and LmForminB FH2 domain are shown in lane 1, 2 along with an empty vector in lane 1. Cloned LmFormins plasmids digestion with BamHI and HindIII leading to expected bands at 1.19kb and 1.3kb. [B] 10% Coomassie-stained SDS-PAGE gel of purified formin A and ForminB protein used in this study. [C, D] The Sensorgram has shown the interaction phase of LmForminA [C] and LmForminB [D], followed by the dissociation phase.

The interaction has been seen by an increase in response in a concentration-dependent manner. [E] Fascin used as a positive control of actin-bundling. [F] SDS-PAGE image of low-speed actin co-sedimentation assay in the presence of the 5 µM actin with different concentration of mutant I777ALmForminA (1µM,2 µM,4 µM). The amount of actin coming in the pellet in the presence of formin represent the actin-bundling activity. [G] SDS-PAGE image of low-speed actin co-sedimentation assay in the presence of the 5 µM actin with different concentration of I802A mutant LmForminB (0.5µM, 1µM, 2µM). The amount of actin coming in the pellet in the presence of formin represent the actin-bundling activity.

**Figure S5. *Leishmania major* formins binding affinity determination with the F-actin.**

[A, B] LmForminA and LmForminB binding affinity with F-actin was determined by the fraction of LmFormins bound to the F-actin. Co-sedimentation assay SDS-PAGE gel image used for the densitometry analysis. [C, D] The dissociation constant determined by the non-linear curve fitting.

**Figure S6. Ile Mutant LmForminA and LmForminB can still inhibit the actin elongation, but lost CapZ replacement activity *in vitro* condition.**

[A, B] 0.5 µM G-actin (10% pyrene-labelled) with F-actin seed used in actin elongation with various concentrations of Mutant LmForminA and LmForminB. LmFormins mixed before the capping protein to see the mutant LmFormins antagonize to capping protein. Actin elongated in the presence of mutant LmFormins, antagonizing the capping protein from the barbed ends.

**Figure S7. LmForminA and LmForminB F-actin-bundling activity is affected in presence high salt concentration.**

[A, B] Coomassie-stained SDS-PAGE of the low-speed pelleting assay using 5µM polymerized actin and increasing concentrations of LmForminA and LmForminB. Only pellets are shown. F-

actin bundling was conducted in polymerization buffer with 50, 100, 150mM KCl final concentration.

**References:**

**Abbasi, K., DuBois, K. N., Dacks, J. B. and Field, M. C.** (2011). A Novel Rho-Like Protein TbRHP Is Involved in Spindle Formation and Mitosis in Trypanosomes. *PLoS ONE* **6**, e26890.

**Ambaru, B., Gopalsamy, A., Satish Tammana, T. V., Subramanya, H. S. and Gupta, C. M.** (2020). Actin sequestering protein, profilin, regulates intracellular vesicle transport in Leishmania. *Molecular and Biochemical Parasitology* **238**, 111280.

**Barkó, S., Bugyi, B., Carlier, M.-F., Gombos, R., Matusek, T., Mihály, J. and Nyitrai, M.** (2010). Characterization of the biochemical properties and biological function of the formin homology domains of Drosophila DAAM. *J. Biol. Chem.* **285**, 13154–13169.

**Baum, J., Tonkin, C. J., Paul, A. S., Rug, M., Smith, B. J., Gould, S. B., Richard, D., Pollard, T. D. and Cowman, A. F.** (2008). A malaria parasite formin regulates actin polymerization and localizes to the parasite-erythrocyte moving junction during invasion. *Cell Host Microbe* **3**, 188–198.

**Castrillon, D. H. and Wasserman, S. A.** (1994). Diaphanous is required for cytokinesis in Drosophila and shares domains of similarity with the products of the limb deformity gene. *Development* **120**, 3367–3377.

**Chalkia, D., Nikolaidis, N., Makalowski, W., Klein, J. and Nei, M.** (2008). Origins and Evolution of the Formin Multigene Family That Is Involved in the Formation of Actin Filaments. *Molecular Biology and Evolution* **25**, 2717–2733.

**Chow, C., Cloutier, S., Dumas, C., Chou, M.-N. and Papadopoulou, B.** (2011). Promastigote to amastigote differentiation of Leishmania is markedly delayed in the absence of PERK eIF2alpha kinase-dependent eIF2alpha phosphorylation. *Cellular Microbiology* **13**, 1059–1077.

**Christensen, J. R., Craig, E. W., Glista, M. J., Mueller, D. M., Li, Y., Sees, J. A., Huang, S., Suarez, C., Mets, L. J., Kovar, D. R., et al.** (2019). Chlamydomonas reinhardtii formin FOR1 and profilin PRF1 are optimized for acute rapid actin filament assembly. *Molecular Biology of the Cell* **30**, 3123–3135.

**Cvrčková, F., Novotný, M., Pícková, D. and Žárský, V.** (2004). Formin homology 2 domains occur in multiple contexts in angiosperms. *BMC Genomics* **5**,.

**Daher, W., Plattner, F., Carlier, M.-F. and Soldati-Favre, D.** (2010). Concerted Action of Two Formins in Gliding Motility and Host Cell Invasion by Toxoplasma gondii. *PLoS Pathogens* **6**, e1001132.

**Daher, W., Klages, N., Carlier, M.-F. and Soldati-Favre, D.** (2012). Molecular Characterization of Toxoplasma gondii Formin 3, an Actin Nucleator Dispensable for Tachyzoite Growth and Motility. *Eukaryotic Cell* **11**, 343–352.

**DeWard, A. D. and Alberts, A. S.** (2009). Ubiquitin-mediated degradation of the formin mDia2 upon completion of cell division. *J. Biol. Chem.* **284**, 20061–20069.

**Dippe, P. von, von Dippe, P. and Levy, D.** (1982). Analysis of the transport system for inorganic anions in normal and transformed hepatocytes. *Journal of Biological Chemistry* **257**, 4381–4385.

**Dutta, P., Das, S. and Maiti, S.** (2017). Non diaphanous formin delphilin acts as a barbed end capping protein. *Exp. Cell Res.* **357**, 163–169.

**Evangelista, M., Pruyne, D., Amberg, D. C., Boone, C. and Bretscher, A.** (2002). Formins direct Arp2/3-independent actin filament assembly to polarize cell growth in yeast. *Nature Cell Biology* **4**, 32–41.

**Filardy, A. A., Guimarães-Pinto, K., Nunes, M. P., Zukeram, K., Fliess, L., Pereira, L., Nascimento, D. O., Conde, L. and Morrot, A.** (2018). Human Kinetoplastid Protozoan Infections: Where Are We Going Next? *Frontiers in Immunology* **9**,.

**Frénal, K. and Soldati-Favre, D.** (2009). Role of the Parasite and Host Cytoskeleton in Apicomplexa Parasitism. *Cell Host & Microbe* **5**, 602–611.

**Gouet, P., Courcelle, E., Stuart, D. and Metoz, F.** (1999). ESPript: analysis of multiple sequence alignments in PostScript. *Bioinformatics* **15**, 305–308.

**Goyard, S., Segawa, H., Gordon, J., Showalter, M., Duncan, R., Turco, S. J. and Beverley, S. M.** (2003). An in vitro system for developmental and genetic studies of Leishmania donovani phosphoglycans. *Molecular and Biochemical Parasitology* **130**, 31–42.

**Gull, K.** (1999). The Cytoskeleton of Trypanosomatid Parasites. *Annual Review of Microbiology* **53**, 629–655.

**Harris, E. S. and Higgs, H. N.** (2006). Biochemical Analysis of Mammalian Formin Effects on Actin Dynamics. *Methods in Enzymology* 190–214.

**Harris, E. S., Li, F. and Higgs, H. N.** (2004). The Mouse Formin, FRLα, Slows Actin Filament Barbed End Elongation, Competes with Capping Protein, Accelerates Polymerization from Monomers, and Severs Filaments. *Journal of Biological Chemistry* **279**, 20076–20087.

**Harris, E. S., Rouiller, I., Hanein, D. and Higgs, H. N.** (2006). Mechanistic differences in actin bundling activity of two mammalian formins, FRL1 and mDia2. *J. Biol. Chem.* **281**, 14383–14392.

**Higgs, H. N. and Pollard, T. D.** (1999). Regulation of Actin Polymerization by Arp2/3 Complex and WASp/Scar Proteins. *Journal of Biological Chemistry* **274**, 32531–32534.

**Ivens, A. C.** (2005). The Genome of the Kinetoplastid Parasite, Leishmania major. *Science* **309**, 436–442.

**Juanes, M. A. and Piatti, S.** (2016). Control of Formin Distribution and Actin Cable Assembly by the E3 Ubiquitin Ligases Dma1 and Dma2. *Genetics* **204**, 205–220.

**Junemann, A., Winterhoff, M., Nordholz, B., Rottner, K., Eichinger, L., Gräf, R. and Faix, J.** (2013). ForC lacks canonical formin activity but bundles actin filaments and is required for multicellular development of Dictyostelium cells. *European Journal of Cell Biology* **92**, 201–212.

**Kato, T., Watanabe, N., Morishima, Y., Fujita, A., Ishizaki, T. and Narumiya, S.** (2001). Localization of a mammalian homolog of diaphanous, mDia1, to the mitotic spindle in HeLa cells. *J. Cell Sci.* **114**, 775–784.

**Kovar, D. R. and Pollard, T. D.** (2004). Insertional assembly of actin filament barbed ends in association with formins produces piconewton forces. *Proceedings of the National Academy of Sciences* **101**, 14725–14730.

**Leong, S. Y., Ong, B. K. T. and Chu, J. J. H.** (2015). The Role of Misshapen NCK-related kinase (MINK), a Novel Ste20 Family Kinase, in the IRES-Mediated Protein Translation of Human Enterovirus 71. *PLOS Pathogens* **11**, e1004686.

**Li, F. and Higgs, H. N.** (2003). The Mouse Formin mDia1 Is a Potent Actin Nucleation Factor Regulated by Autoinhibition. *Current Biology* **13**, 1335–1340.

**Li, F. and Higgs, H. N.** (2005). Dissecting Requirements for Auto-inhibition of Actin Nucleation by the Formin, mDia1. *Journal of Biological Chemistry* **280**, 6986–6992.

**Li, M.-Y., Peng, W.-H., Wu, C.-H., Chang, Y.-M., Lin, Y.-L., Chang, G.-D., Wu, H.-C. and Chen, G.-C.** (2019). PTPN3 suppresses lung cancer cell invasiveness by counteracting Src-mediated DAAM1 activation and actin polymerization. *Oncogene* **38**, 7002–7016.

**Lu, J., Meng, W., Poy, F., Maiti, S., Goode, B. L. and Eck, M. J.** (2007). Structure of the FH2 domain of Daam1: implications for formin regulation of actin assembly. *J. Mol. Biol.* **369**, 1258–1269.

**Maas, R. L., Zeller, R., Woychik, R. P., Vogt, T. F. and Leder, P.** (1990). Disruption of formin-encoding transcripts in two mutant limb deformity alleles. *Nature* **346**, 853–855.

**Majumder, S. and Lohia, A.** (2008). Entamoeba histolytica Encodes Unique Formins, a Subset of Which Regulates DNA Content and Cell Division. *Infection and Immunity* **76**, 2368–2378.

**McConville, M. J., Mullin, K. A., Ilgoutz, S. C. and Teasdale, R. D.** (2002). Secretory Pathway of Trypanosomatid Parasites. *Microbiology and Molecular Biology Reviews* **66**, 122–154.

**Michelot, A., Guérin, C., Huang, S., Ingouff, M., Richard, S., Rodiuc, N., Staiger, C. J. and Blanchoin, L.** (2005). The Formin Homology 1 Domain Modulates the Actin Nucleation and Bundling Activity of Arabidopsis FORMIN1. *The Plant Cell* **17**, 2296–2313.

**Moseley, J. B. and Goode, B. L.** (2005). Differential Activities and Regulation of Saccharomyces cerevisiae Formin Proteins Bni1 and Bnr1 by Bud6. *Journal of Biological Chemistry* **280**, 28023–28033.

**Moseley, J. B., Maiti, S. and Goode, B. L.** (2006). Formin Proteins: Purification and Measurement of Effects on Actin Assembly. *Methods in Enzymology* 215–234.

**Nayak, R. C., Sahasrabuddhe, A. A., Bajpai, V. K. and Gupta, C. M.** (2005). A novel homologue of coronin colocalizes with actin in filament-like structures in Leishmania. *Molecular and Biochemical Parasitology* **143**, 152–164.

**Okwor, I. and Uzonna, J.** (2016). Social and Economic Burden of Human Leishmaniasis. *The American Journal of Tropical Medicine and Hygiene* **94**, 489–493.

**Ozaki-Kuroda, K., Yamamoto, Y., Nohara, H., Kinoshita, M., Fujiwara, T., Irie, K. and Takai, Y.** (2001). Dynamic Localization and Function of Bni1p at the Sites of Directed Growth in Saccharomyces cerevisiae. *Molecular and Cellular Biology* **21**, 827–839.

**Pal, D. S., Mondal, D. K. and Datta, R.** (2015). Identification of Metal Dithiocarbamates as a Novel Class of Antileishmanial Agents. *Antimicrobial Agents and Chemotherapy* **59**, 2144–2152.

**Patel, A. A., Oztug Durer, Z. A., van Loon, A. P., Bremer, K. V. and Quinlan, M. E.** (2018). Drosophila and human FHOD family formin proteins nucleate actin filaments. *Journal of Biological Chemistry* **293**, 532–540.

**Petersen, J., Nielsen, O., Egel, R. and Hagan, I. M.** (1998). FH3, A Domain Found in Formins, Targets the Fission Yeast Formin Fus1 to the Projection Tip During Conjugation. *Journal of Cell Biology* **141**, 1217–1228.

**Pollard, T. D.** (1984). Polymerization of ADP-actin. *Journal of Cell Biology* **99**, 769–777.

**Ponte-Sucre, A., Gamarro, F., Dujardin, J.-C., Barrett, M. P., López-Vélez, R., García-Hernández, R., Pountain, A. W., Mwenechanya, R. and Papadopoulou, B.** (2017). Drug resistance and treatment failure in leishmaniasis: A 21st century challenge. *PLOS Neglected Tropical Diseases* **11**, e0006052.

**Pruyne, D.** (2002). Role of Formins in Actin Assembly: Nucleation and Barbed-End Association. *Science* **297**, 612–615.

**Rivero, F., Muramoto, T., Meyer, A.-K., Urushihara, H., Uyeda, T. Q. P. and Kitayama, C.** (2005). A comparative sequence analysis reveals a common GBD/FH3-FH1-FH2-DAD architecture in formins from Dictyostelium, fungi and metazoa. *BMC Genomics* **6**,.

**Rizvi, S. A., Neidt, E. M., Cui, J., Feiger, Z., Skau, C. T., Gardel, M. L., Kozmin, S. A. and Kovar, D. R.** (2009). Identification and characterization of a small molecule inhibitor of formin-mediated actin assembly. *Chem. Biol.* **16**, 1158–1168.

**Romero, S., Didry, D., Larquet, E., Boisset, N., Pantaloni, D. and Carlier, M.-F.** (2007). How ATP Hydrolysis Controls Filament Assembly from Profilin-Actin. *Journal of Biological Chemistry* **282**, 8435–8445.

**Sagot, I., Klee, S. K. and Pellman, D.** (2002). Yeast formins regulate cell polarity by controlling the assembly of actin cables. *Nature Cell Biology* **4**, 42–50.

**Sahasrabuddhe, A. A., Bajpai, V. K. and Gupta, C. M.** (2004). A novel form of actin in Leishmania: molecular characterisation, subcellular localisation and association with subpellicular microtubules. *Molecular and Biochemical Parasitology* **134**, 105–114.

**Sahasrabuddhe, A. A., Nayak, R. C. and Gupta, C. M.** (2009). Ancient Leishmania coronin (CRN12) is involved in microtubule remodeling during cytokinesis. *Journal of Cell Science* **122**, 1691–1699.

**Schonichen, A., Mannherz, H. G., Behrmann, E., Mazur, A. J., Kuhn, S., Silvan, U., Schoenenberger, C.-A., Fackler, O. T., Raunser, S., Dehmelt, L., et al.** (2013). FHOD1 is a combined actin filament capping and bundling factor that selectively associates with actin arcs and stress fibers. *Journal of Cell Science* **126**, 1891–1901.

**Scott, B. J., Neidt, E. M. and Kovar, D. R.** (2011). The functionally distinct fission yeast formins have specific actin-assembly properties. *Molecular Biology of the Cell* **22**, 3826–3839.

**Shi, L., Huo, J.-W., Chen, S.-S., Xue, J.-X., Gao, W.-Y., Li, X.-Y., Song, Y.-H., Xu, H.-T., Zhu, X.-W. and Chen, K.** (2019). MicroRNA-22 targets FMNL2 to inhibit melanoma progression via the regulation of the Wnt/β-catenin signaling pathway and epithelial-mesenchymal transition. *Eur. Rev. Med. Pharmacol. Sci.* **23**, 5332–5342.

**Shimada, A., Nyitrai, M., Vetter, I. R., Kühlmann, D., Bugyi, B., Narumiya, S., Geeves, M. A. and Wittinghofer, A.** (2004). The core FH2 domain of diaphanous-related formins is an elongated actin binding protein that inhibits polymerization. *Mol. Cell* **13**, 511–522.

**Silkworth, W. T., Kunes, K. L., Nickel, G. C., Phillips, M. L., Quinlan, M. E. and Vizcarra, C. L.** (2018). The neuron-specific formin Delphilin nucleates nonmuscle actin but does not enhance elongation. *Molecular Biology of the Cell* **29**, 610–621.

**Skillman, K. M., Daher, W., Ma, C. I., Soldati-Favre, D. and Sibley, L. D.** (2012). Toxoplasma gondii profilin acts primarily to sequester G-actin while formins efficiently nucleate actin filament formation in vitro. *Biochemistry* **51**, 2486–2495.

**Stortz, J. F., Del Rosario, M., Singer, M., Wilkes, J. M., Meissner, M. and Das, S.** (2019). Formin-2 drives polymerisation of actin filaments enabling segregation of apicoplasts and cytokinesis in Plasmodium falciparum. *eLife* **8**,.

**Sunter, J. and Gull, K.** (2017). Shape, form, function and Leishmania pathogenicity: from textbook descriptions to biological understanding. *Open Biology* **7**, 170165.

**Tammana, T. V. S., Sahasrabuddhe, A. A., Bajpai, V. K. and Gupta, C. M.** (2010). ADF/cofilin-driven actin dynamics in early events of Leishmania cell division. *Journal of Cell Science* **123**, 1894–1901.

**Thumkeo, D., Katsura, Y., Nishimura, Y., Kanchanawong, P., Tohyama, K., Ishizaki, T., Kitajima, S., Takahashi, C., Hirata, T., Watanabe, N., et al.** (2020). mDia1/3-dependent actin polymerization spatiotemporally controls LAT phosphorylation by Zap70 at the immune synapse. *Science Advances* **6**, eaay2432.

**Tosetti, N., Dos Santos Pacheco, N., Soldati-Favre, D. and Jacot, D.** (2019). Three F-actin assembly centers regulate organelle inheritance, cell-cell communication and motility in Toxoplasma gondii. *eLife* **8**,.

**Tsigankov, P., Gherardini, P. F., Helmer-Citterich, M., Späth, G. F., Myler, P. J. and Zilberstein, D.** (2014). Regulation Dynamics of Leishmania Differentiation: Deconvoluting Signals and Identifying Phosphorylation Trends. *Molecular & Cellular Proteomics* **13**, 1787–1799.

**Vasconcelos, E. J. R., Pacheco, A. C. L., Gouveia, J. J. S., Araujo, F. F., Diniz, M., Kamimura, M., Costa, M., Araujo-Filho, R. and Oliveira, D.** (2008). Actin-Interacting Proteins in flagellated pathogenic Leishmania spp.: a genome-based bioinformatics report on profilins, formins and katanins. *Int. J. Funct. Inform. Personal. Med.* **1**, 234–252.

**Wasserman, S.** (1998). FH proteins as cytoskeletal organizers. *Trends in Cell Biology* **8**, 111–115.

**Xu, Y., Moseley, J. B., Sagot, I., Poy, F., Pellman, D., Goode, B. L. and Eck, M. J.** (2004). Crystal Structures of a Formin Homology-2 Domain Reveal a Tethered Dimer Architecture. *Cell* **116**, 711–723.

**Yamashiro, S., Yamakita, Y., Ono, S. and Matsumura, F.** (1998). Fascin, an Actin-bundling Protein, Induces Membrane Protrusions and Increases Cell Motility of Epithelial Cells. *Molecular Biology of the Cell* **9**, 993–1006.

**Yang, J., Zhou, L., Zhang, Y., Zheng, J., Zhou, J., Wei, Z. and Zou, J.** (2019). DIAPH1 Is Upregulated and Inhibits Cell Apoptosis through ATR/p53/Caspase-3 Signaling Pathway in Laryngeal Squamous Cell Carcinoma. *Dis. Markers* **2019**, 6716472.

**Zeller, R., Haramis, A. G., Zuniga, A., McGuigan, C., Dono, R., Davidson, G., Chabanis, S. and Gibson, T.** (1999). Formin defines a large family of morphoregulatory genes and functions in establishment of the polarising region. *Cell and Tissue Research* **296**, 85–93.

**Zilberstein, D.** (2015). Proteomic Analysis of Posttranslational Modifications Using iTRAQ in Leishmania. *Methods in Molecular Biology* 261–268.

**Zimmermann, D., Morganthaler, A. N., Kovar, D. R. and Suarez, C.** (2016). In Vitro Biochemical Characterization of Cytokinesis Actin-Binding Proteins. *Methods in Molecular Biology* 151–179.

**Ziske, M. A., Pettee, K. M., Khaing, M., Rubinic, K. and Eisenmann, K. M.** (2016). SMIFH2-mediated mDia formin functional inhibition potentiates chemotherapeutic targeting of human ovarian cancer spheroids. *Biochem. Biophys. Res. Commun.* **472**, 33–39.

**Figure 1**

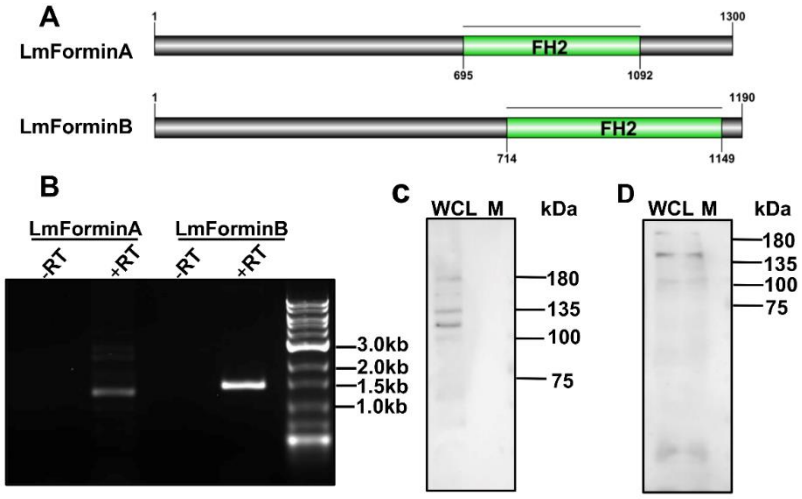

951

**Figure 2**

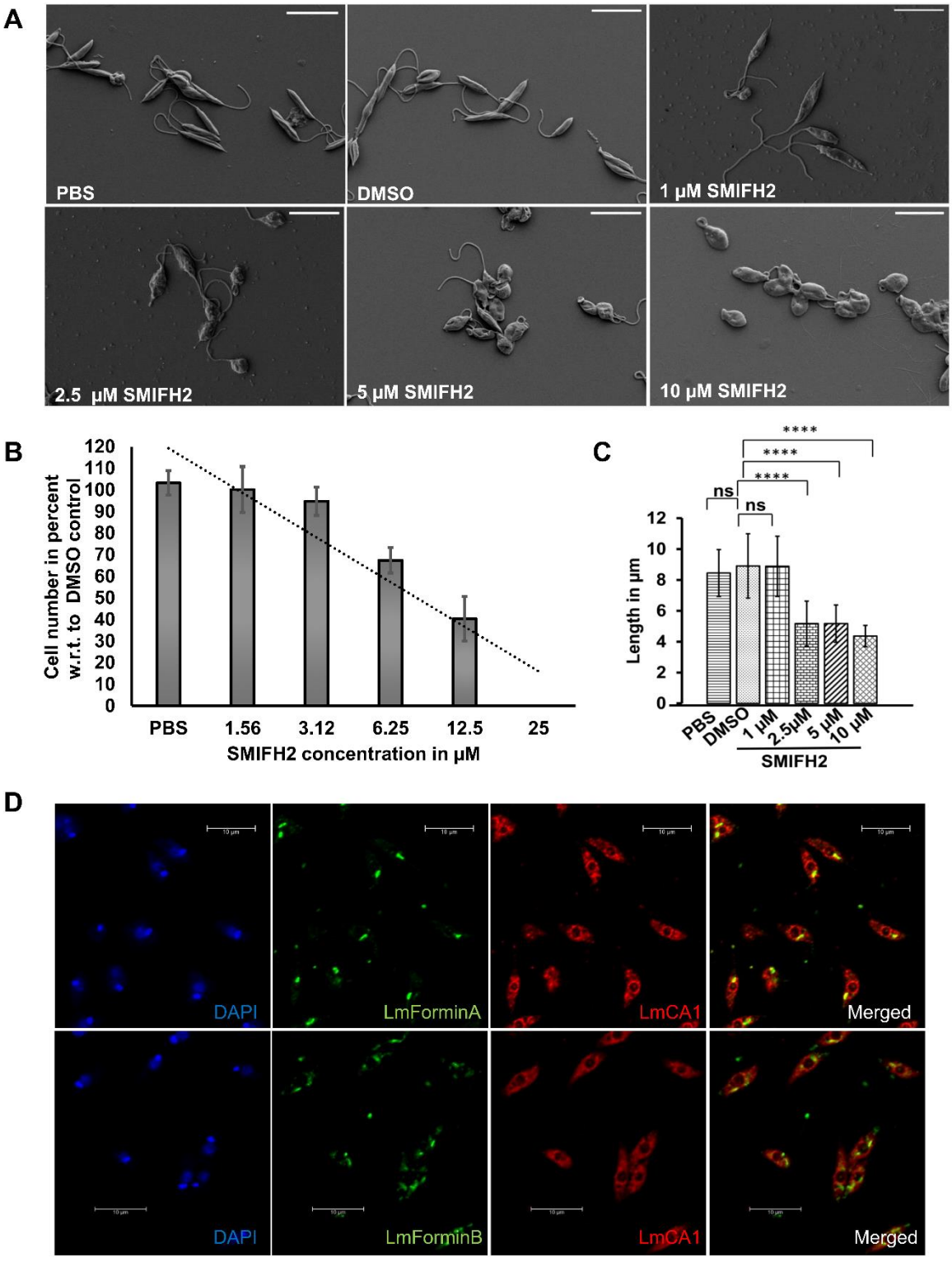


952

953

**Figure 3**

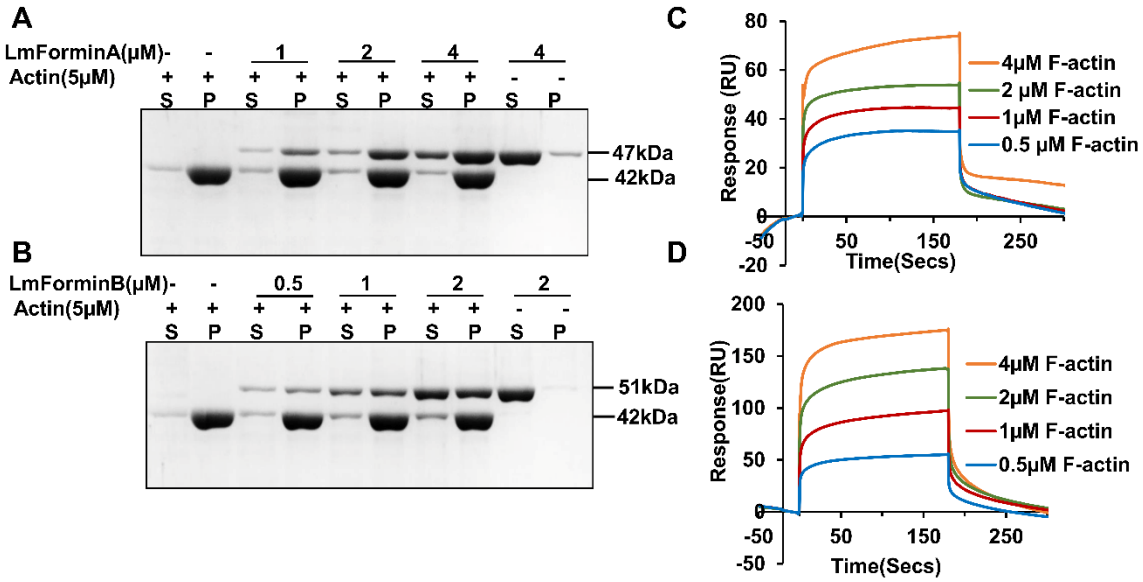


954

955

**Figure 4**

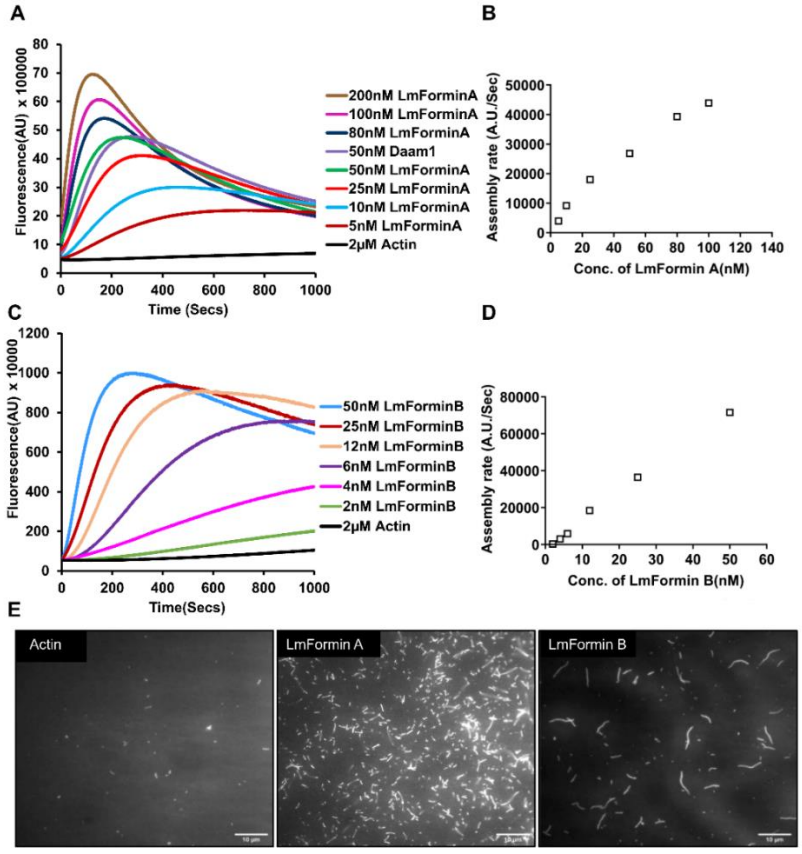


956

957

**Figure 5**

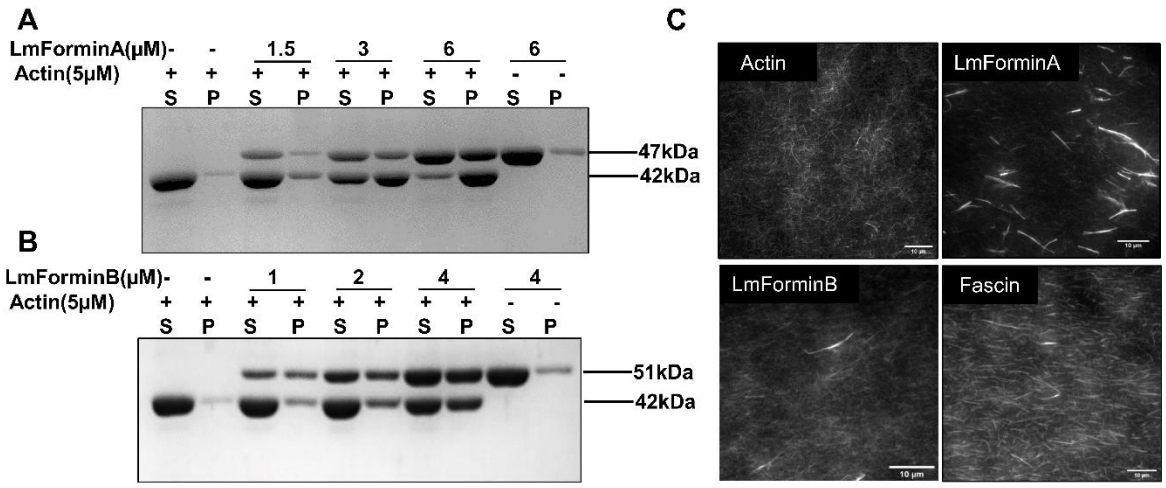


958

959

960

961

962

963

964

965

966

967

968

969

970

971

972

973

974

**Figure 6**

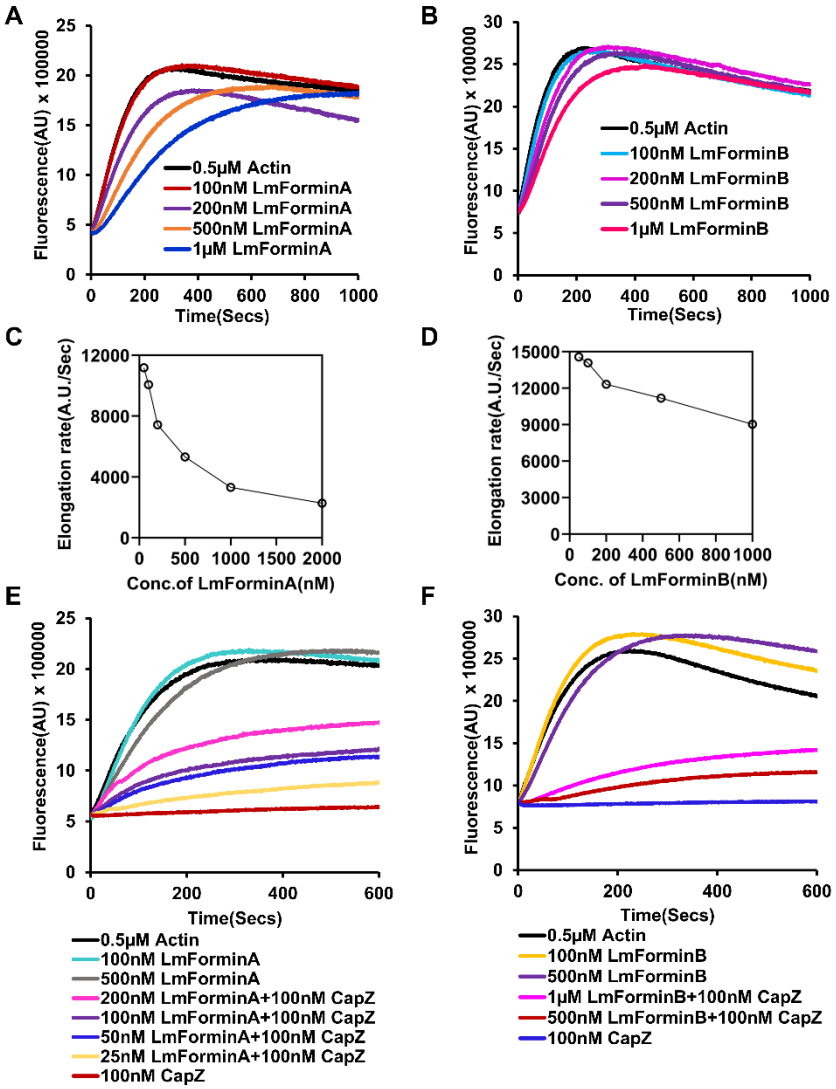


975

976

977

978

979

980

981

982

983

984 **Figure 7**

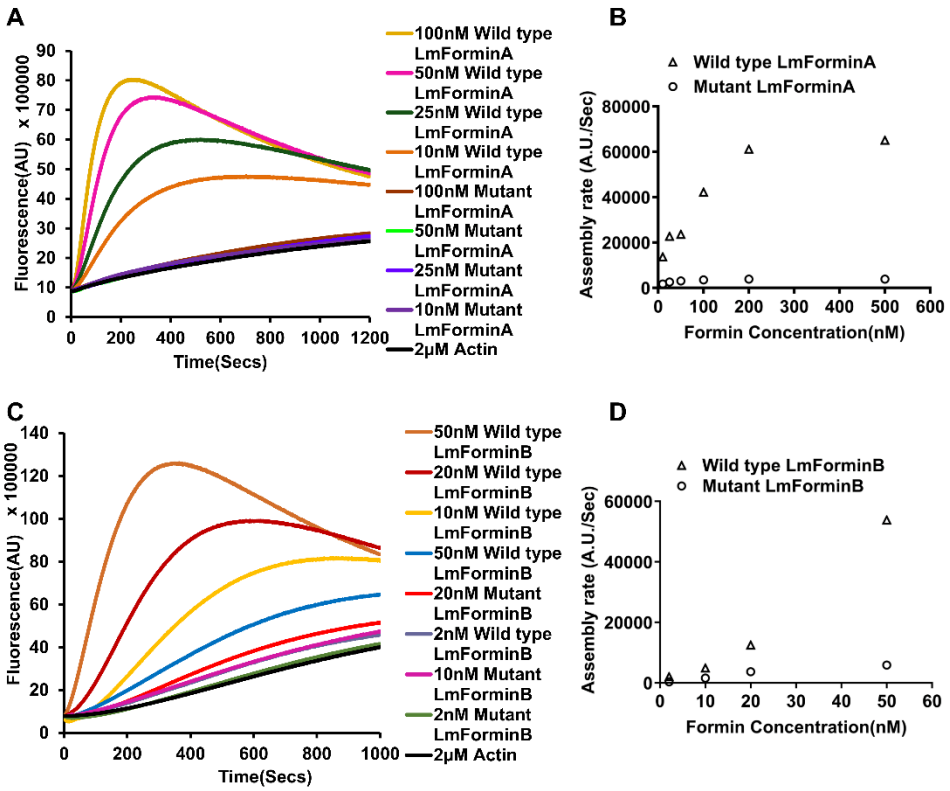


985 **Figure S1**

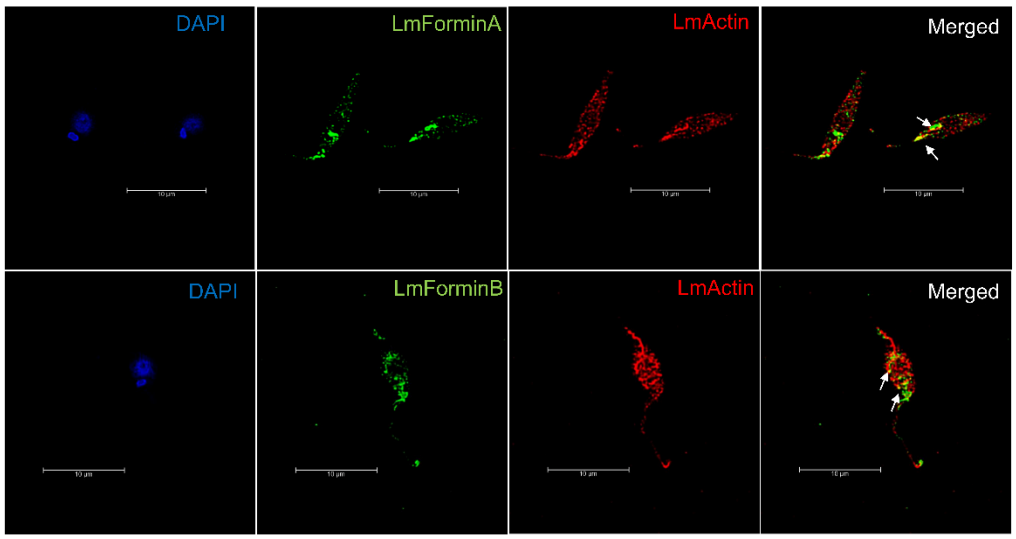


986 **Figure S2**

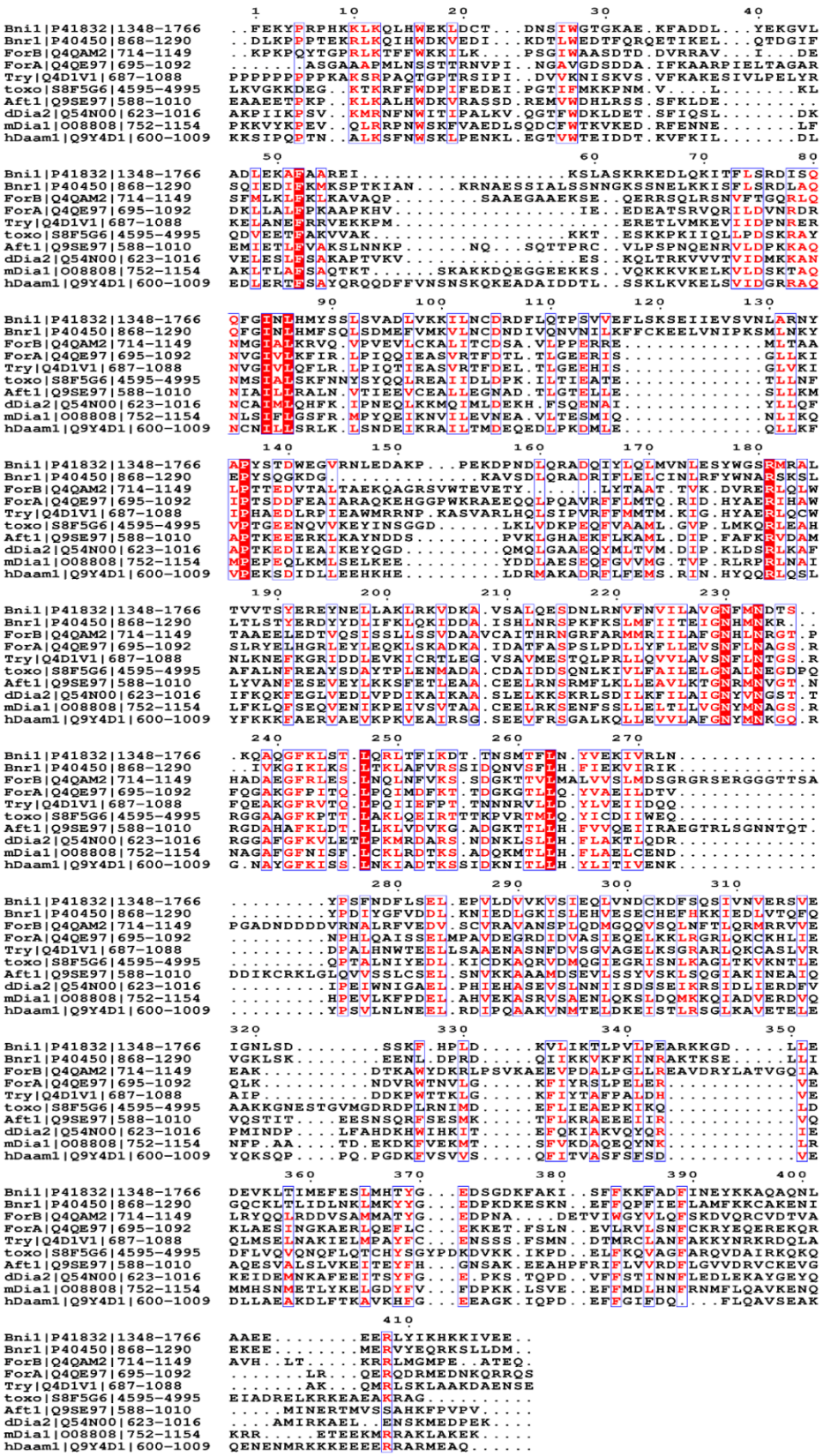

988

**Figure S3**

| LmForminA | | | | LmForminB | | | |
|---|---|---|---|---|---|---|---|
| **Formin** | **Species** | **Identity** | **Similarity** | **Formin** | **Species** | **Identity** | **Similariy** |
| TC00 | *T. cruzi* | 40.9% | 57% | TC00 | *T. cruzi* | 18.1% | 34.8% |
| Bni1 | *S.cerevisiae* | 23.2% | 40.1% | Bni1 | *S.cerevisiae* | 21.3% | 35.3% |
| Bnr1 | *S.cerevisiae* | 17.9% | 33.5% | Bnr1 | *S.cerevisiae* | 20.6% | 36.9% |
| cdc12 | *S.pombe* | 20.1% | 37.0% | cdc12 | *S.pombe* | 19.1% | 36.1% |
| dDia2 | *D.discoideum* | 24.7% | 44.8% | dDia2 | *D. discoideum* | 20.7% | 39.0% |
| AFH1 | *A.thaliana* | 22.3% | 42.1% | AFH1 | *A.thaliana* | 24.2% | 43.5% |
| mDia1 | *M.musculus* | 20.8% | 36.1% | mDia1 | *M. musculus* | 21.8% | 39.7 |
| Daam1 | *H.sapiens* | 22.6% | 44.2% | Daam1 | *H.sapiens* | 21.4% | 42.6% |

989

990

**Figure S4**

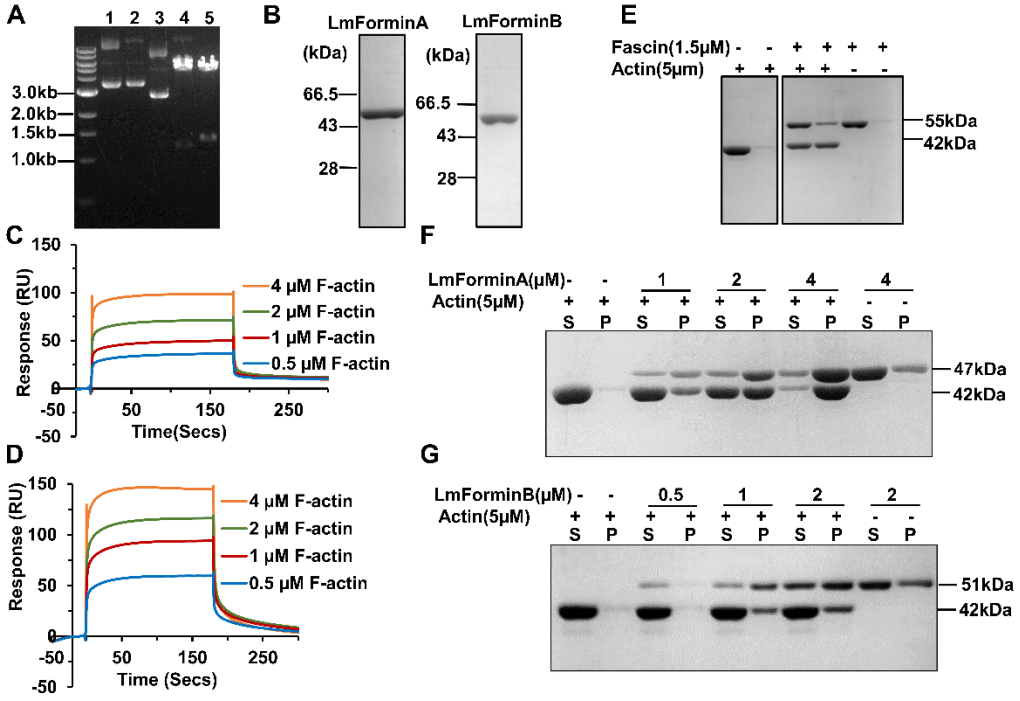


991

992

**Figure S5**

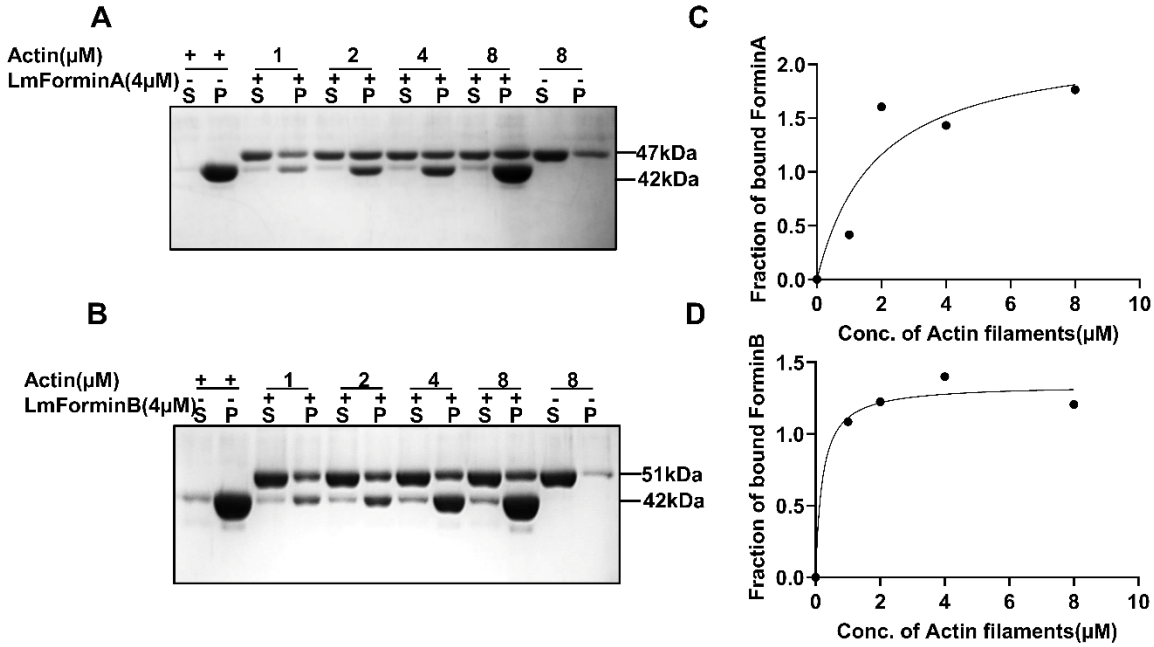


993

994

**Figure S6**

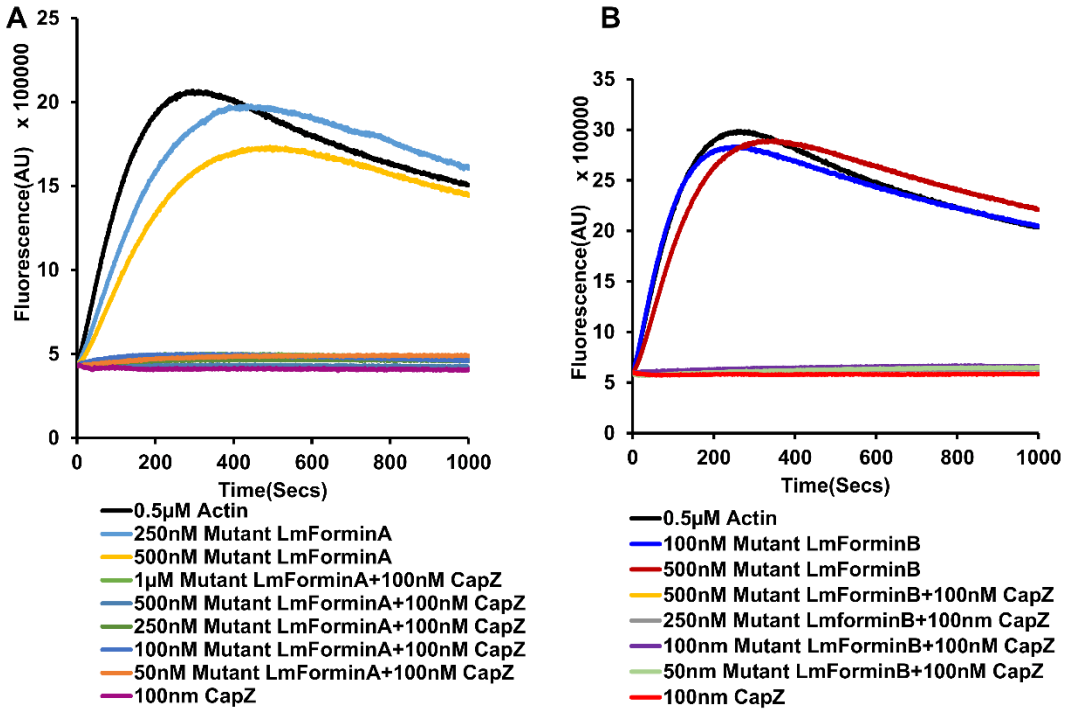


995

996

997 **Figure S7**

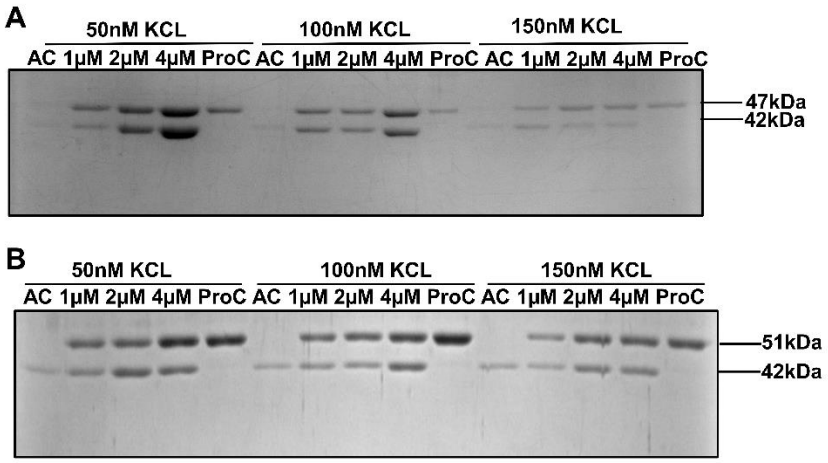


998